EurJOC
European Journal of Organic Chemistry

Review
doi.org/10.1002/ejoc.202201360

Chemistry
Europe
European Chemical
Societies Publishing

www.eurjoc.org

Design, Synthesis, and Biomedical Applications of Glycotripods for Targeting Trimeric Lectins

Vinod Khatri,[a, b] Badri Parshad,[c] Ashok K. Prasad,[d] and Sumati Bhatia*[a]

In the last decades, various efforts have been made to synthesize optimal glycotripods for targeting trimeric glycoproteins like asialoglycoprotein receptor, hemagglutinin, and langerin. All these trimeric glycoproteins have sugar binding pockets which are highly selective for a particular carbohydrate ligand. Optimized glycotripods are high affinity binders and have been used for delivering drugs or even applied as drug candidates. The selection of the tripodal base scaffold together with the length and flexibility of the linker between the scaffold and sugar residue, as important design parameters are discussed in this review.

1. Introduction

Carbohydrate-protein interactions play an important role in the binding of pathogens to the host cell surface.[1] These interactions are involved in the development of various diseases, such as pathogen infection, inflammation, and tumor metathesis.[2] In a biological system, carbohydrates are mainly present in the form of glycoproteins, glycolipids, starch, and cellulose.[3] All cell surfaces are covered with glycocalyx which is made of glycolproteins and glycolipids. The glycocalyx connects the inner side of the cell with its outer side and is hence involved in various biological processes including cell-cell communication. Also, carbohydrate residues of cell surface glycocalyx interact with other glyco-residues and various lectins to initiate biological responses.[4] During these interactions, the polar hydroxyl groups of carbohydrates bind with the polar amino acid residue of lectin primarily through hydrogen bonding and the hydrophobic part of glycoconjugates binds with the hydrophobic part (aromatic ring) of lectin protein through hydrophobic-hydrophobic and π-π interactions.[5] Monovalent carbohydrate has a weak binding with lectin protein and therefore, has limited biological significance. Lectins are in general multivalent, and therefore multivalent carbohydrate ligands have been proposed and explored as high affinity binders of various lectins with an increase in binding affinities from mM to nM or pM range.[6–11] However, a controlled and specific design of an accurately binding multivalent ligand is highly challenging. This requires the selection of a proper scaffold, linker, and ligand. Differently designed glycotripods have been materialized to study their binding effects with trimeric lectins.[12,13] These designs are based on the spatial orientation of binding pockets on the receptor protein. Numerous reviews have been published on the topic of multivalent glycosides which mainly focused on carbohydrate-proteins interactions,[14] multivalent glycoconjugates,[15] and multivalent ligands for targeting hepatocytes.[16] This review article particularly emphasized on the synthesis of trivalent architectures for targeting trimeric lectins such as asialoglyco-protein, hemagglutinin, and langerin. Moreover, other trivalent glycosides which are targeting plant lectin, such as concanavalin A, gram negative bacteria such as *E. coli*, and adenovirus (Ad37) have also been summarized in the miscellaneous section of this review.

2. Asialoglycoprotein Receptor

The asialoglycoprotein receptor (ASGPR), also known as the Ashwell-Morell receptor is a heterooligomeric *C*-type (calcium dependent) hepatic lectin overexpressed on hepatocytes. The main function of this receptor is to maintain serum glycoprotein homeostasis by recognition, binding, and endocytosis of asialoglycoproteins (desialylated glycoproteins with *N*-acetyl galactosamine and galactose residues at terminal positions). ASGPR-mediated endocytosis is a reversible process and the receptor recycles again on the cell surface in 15 minutes.[17] The *N*-acetyl galactosamine has a higher binding affinity for ASGPR than galactose. Calcium ion is the prerequisite for proper recognition and binding of glyco-ligand to the receptor. The

[a] Dr. V. Khatri, Dr. S. Bhatia
    Institute for Chemistry and Biochemistry
    Freie University Berlin
    Takustr. 3, Berlin 14195 (Germany)
    E-mail: sumati@zedat.fu-berlin.de
[b] Dr. V. Khatri
    Department of Chemistry
    TDL Govt. College for Women
    Murthal 131027, Sonipat, Haryana (India)
[c] Dr. B. Parshad
    Wellman Center for Photomedicine
    Massachusetts General Hospital
    Harvard Medical School
    Boston, MA 02129 (USA)
[d] Prof. A. K. Prasad
    Bioorganic Laboratory
    Department of Chemistry
    University of Delhi
    Delhi 110007 (India)

EurJOC
European Journal of Organic Chemistry

Review
doi.org/10.1002/ejoc.202201360

Chemistry Europe
European Chemical
Societies Publishing

receptor binding is sensitive to pH and the receptor-ligand complex dissociates in low pH in endosomes and the receptor recycles back to the cell surface. The hepatic infections are mediated by ASGPR because hepatitis A and hepatitis B viruses bind to this receptor and hence led to infection.[18] ASGPR has been widely explored for the targeted delivery of chemically modified nucleotides, siRNA,[19] and drugs to the hepatocytes.[8]

The ASGPR has two homologous major and minor subunits with two distinct genes. In humans, the major subunit is H1 having a molecular weight of 46 kDa and the minor subunit is H2 having a molecular weight of 50 kDa with 55% sequence identity. The cell lines expressing only H1 or H2 are unable to bind with ligand because the expression of both subunits is required for the endocytosis of ligand.[20] The general structure of human ASGPR can be subdivided into four functional domains: Cytosolic domain having N-terminal 40 amino acids, the single-pass transmembrane domain having 20 amino acids, the extracellular stalk region has 80 amino acids and 140 amino acids functional calcium dependent carbohydrate recognition domain (CRD).[21] The sugar binding sites of the ASGPR are estimated to be 15–25 Å apart in a triangle spatial geometry. It has been reported that the galactose cluster with a 20 Å spacer exhibited a 2000-fold higher affinity for ASGPR than the galactose cluster lacking the spacer.[22] The important factors for the design of multivalent ligands for targeting ASGPR are linker length, the hydrophilic-hydrophobic balance of the linker, the nature, and a number of terminal sugar units, and the spatial geometry of the scaffold (Figure 1). The trivalent glycoconjugates are mainly derived from peptide and dendrimeric scaffolds. Among various dendrimeric scaffolds, tris(hydroxymethyl)aminomethane (Tris) is the most commonly used scaffold for the design of trivalent glycoconjugates for targeting ASGPR.

In 1987, Lee and coworkers[23] have synthesized glutamic acid based dimeric and trimeric glycosides with two and three N-acetyl galactosylamine groups at the terminal position. For the synthesis of trimeric glycoside, the three carboxyl groups of γ-L-glutamyl-L-glutamic acid (γ-EE) were derivatized by coupling of Z-Tyrosine to glutamyl-L-glutamic acid to afford Z-Tyr-Glu-Glu (ZYEE) followed by the coupling of GalNAcAH (6-aminohexyl-2-acetamido-2-deoxy-β-D-galactopyranoside) and Lac-AH (6-aminohexyl-β-lactopyranoside) with ZYEE to afford ZYEE(GalNAc-AH)$_3$ and ZYEE(Lac-AH)$_3$. Removal of the Z-group by hydrogenolysis led to the synthesis of YEE(GalNAc-AH)$_3$ and YEE(Lac-AH)$_3$ (Figure 2A). Among various synthesized cluster glycosides, the trimeric glycolconjugate was the most potent in rat hepatocyte surface binding. The IC$_{50}$ of trimeric glycolconjugate (0.2 nM) was 15 times lower than the corresponding dimeric glycoconjugate (3 nM) as determined by the inhibition assay with Asialooorosomucoid (^{125}I-ASOR) in rat hepatocytes. Furthermore, The IC$_{50}$ value of YEE(Lac-AH)$_3$ was 50 nM which is 250 folds higher than the YEE(GalNAc-AH)$_3$. It was observed that the strongest binding can be achieved by long and flexible arms between the main scaffold and the N-acetyl galactosylamine.

In the solution phase synthesis of YEE(GalNAc-AH)$_3$, the solubility of the intermediates formed was not good. Hence, to solve the solubility problem of intermediate in the synthesis of

Vinod Khatri studied Chemistry at Kurukshetra University, Haryana, India and received his Ph.D. from University of Delhi under the supervision of Professor Ashok K. Prasad. After Ph.D. in 2017, he joined IISER Mohali as National Postdoctoral Fellow (DST-SERB) and worked on metal-catalyzed reactions on carbohydrates. In 2018, he joined the Department of Higher Education Haryana as an Assistant Professor. In 2021, he worked as a postdoctoral fellow at Freie Universität Berlin, Germany for one year with Dr. Sumati Bhatia. His research interests focus on C-glycosides, sugar-based copolymers, and multivalent glycoconjugates.

Badri Parshad received his M.Sc. in 2011 from the Kurukshetra University, India, and his Ph.D. in chemistry from the University of Delhi under the supervision of Professor Sunil K. Sharma. Thereafter, he moved to the Freie Universität Berlin, Germany in 2018 and to the University of Cambridge, UK in 2019, and worked as a postdoctoral researcher. He joined the Massachusetts General Hospital, Harvard Medical School, USA as a research fellow in 2022. His research interests include organic and polymer chemistry, drug delivery nanocarriers, multivalent pathogen inhibitors as well as sensing materials for pH, oxygen, and carbon dioxide.

Ashok K. Prasad obtained his Ph.D. from Department of Chemistry, University of Delhi in 1990 in the area of synthesis of bioactive polyphenolic natural products. After spending about a decade as a post-doctoral fellow/visiting scientist at the University of Southern Denmark, the Max Planck Institute for Molecular Physiology (Germany), Sapienza University Rome (Italy) and the University of Massachusetts Lowell (USA), Professor Prasad joined the Department of Chemistry, University of Delhi as Reader in 2001 and subsequently became Professor in 2009. His research interest lies in the areas of nucleic acid chemistry, biotransformations, natural product chemistry, and synthesis of bioactive heterocyclic compounds.

Sumati Bhatia studied Chemistry at the University of Delhi, India. After receiving Ph.D. in Organic Chemistry at the University of Delhi (Prof. Ashok K. Prasad), India in 2012, she joined as a postdoc at Freie Universität Berlin (Prof. Rainer Haag), Germany. She was leading a subgroup in FUB until she started her own position as a group leader in 2020. She has leading expertise in different glycoarchitectures and is interested in developing new technologies for combating viral and bacterial infections.
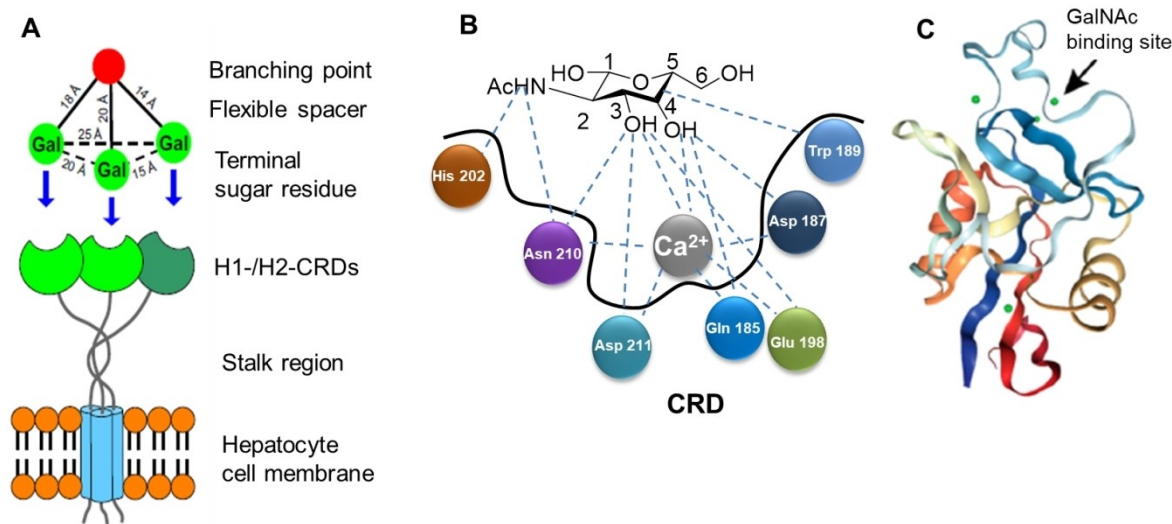
EurJOC
European Journal of Organic Chemistry

Review
doi.org/10.1002/ejoc.202201360

Chemistry
Europe
European Chemical
Societies Publishing

Figure 1. (A) Binding model for ASGPR ligands in an optimal conformation. Reproduced with permission from Ref. [37]. Copyright (2008), Elsevier; (B) Binding of GalNAc to the CRD. (C) Crystal structure of H1-CRD; Figures B and C are Reproduced with permission from Ref. [16]. Copyright (2017), American Chemical Society.

YEE(GalNAc-AH)$_3$, Chen and co-workers[24] synthesized the YEE-(GalNAc-AH)$_3$ by solid phase method in several steps. This synthetic procedure permits the conjugation of drugs or another compound on the *N*-terminal end of tyrosine. Resin amine was used as solid support to conjugate the *N*-acetyl galactosamine through succinic acid linker **2b**. After conjugation of N-acetylgalactosamine, Fmoc was removed using 20% piperidine, and compound **2a** was coupled twice followed by Fmoc deprotection. Further, coupling of Fmoc-Tyr-OH, deprotection of Fmoc, and removal of resin and acetyl groups of sugar units was done to obtain the desired product YEE-(GalNAc-AH)$_3$ (Figure 2B). As the preparation of YEE(GalNAc-AH)$_3$ had some practical problems due to the poor solubility of the peptide backbone. In 1997, Lee and coworkers[25] reported the method for the synthesis of YDD(G-AH-GalNAc)$_3$ which is a homologous glycoconjugate of YEE(GalNAc-AH)$_3$ (Figure 2C). The EE peptide backbone was replaced by β-L-aspartyl-L-aspartic acid (β-DD) peptide and a glycine unit was added which improves the synthetic protocol and requires no chromatographic purification. Moreover, the IC$_{50}$ of the new trivalent ligand was comparable to the YEE(GalNAc-AH)$_3$.

In 1997, van Boom and coworkers[26] synthesized the lysyl-lysine dipeptide based cluster galactosides via multistep solid support synthesis. For this synthesis, sugar building blocks were prepared in various steps. The 4-(hydroxymethyl)benzoic acid (HMBA) functionalized resin was used to couple the first amino acid Fmoc-Lys(Alloc)-OH. Further, after deprotection of amine, galactose derivative was coupled to afford lysine mono-saccharide adduct. The lysine monosaccharide adduct was coupled with another lysine unit to obtain the lys-lys mono-saccharide adduct. After the deprotection of two amines, lys-lys monosaccharide was coupled with two galactose derivatives followed by the removal of solid support to afford the desired product (Figure 3A). The binding affinity of lysine based

galactosides **3a**–**3d** for ASGPR was determined by inhibitory assay with ^{125}I-ASOR. It is clear from the Table in Figure 3A that galactose terminal glycoconjugate (**3a**) has many fold less binding affinity than their corresponding *N*-acetyl galactos-amine terminal glycoconjugates (**3b**). The incorporation of glycine unit (compound **3c**) led to a slight decrease in the binding affinity. Moreover, the incorporation of γ-aminobutyric acid (compound **3d**) has a small effect on the binding affinity. It was concluded that lysine-based *N*-acetyl galactosamine con-jugates have no significant effect on spacer length.

In 1995, Biessen et al. synthesized adipic acid based trivalent galactosides with various spacer lengths between terminal galactose and the branching point of dendrite.[27] The dendrite Tris was coupled with glycine and adipic acid to obtain compound **3e**. Compound **3e** was further coupled with galactosides having linkers of different lengths to afford the desired compounds **3f**–**3j** (Figure 3B). The affinity of synthe-sized trivalent galactosides with ASGPR was determined by competitive studies of ^{125}I-ASOR binding. It has been observed that the binding affinity increases manyfold with an increase in the spacer length. The binding affinity of trivalent galactoside **3j** having the longest spacer is almost 2000 fold higher than the corresponding galactoside with a small spacer **3f**. However, trivalent galactosides with a medium size spacer (9, 10, and 13 Å) show 20–300 fold intermediate binding affinity as compared to small spacer galactoside. The trivalent galactoside with 10 Å spacer, TG (10 Å) shows 10-fold higher affinity than TG (9 and 13 Å) which could arise from the enhanced hydro-phobicity of 1-propyl unit of the terminal galactose unit as compared to 1-ethyl unit in TG (9 and 13 Å). It is evident that an increase in hydrophobicity near the galactose unit led to a significant increase in the binding affinity. Further, it was concluded that the galactose units of trivalent galactosides are
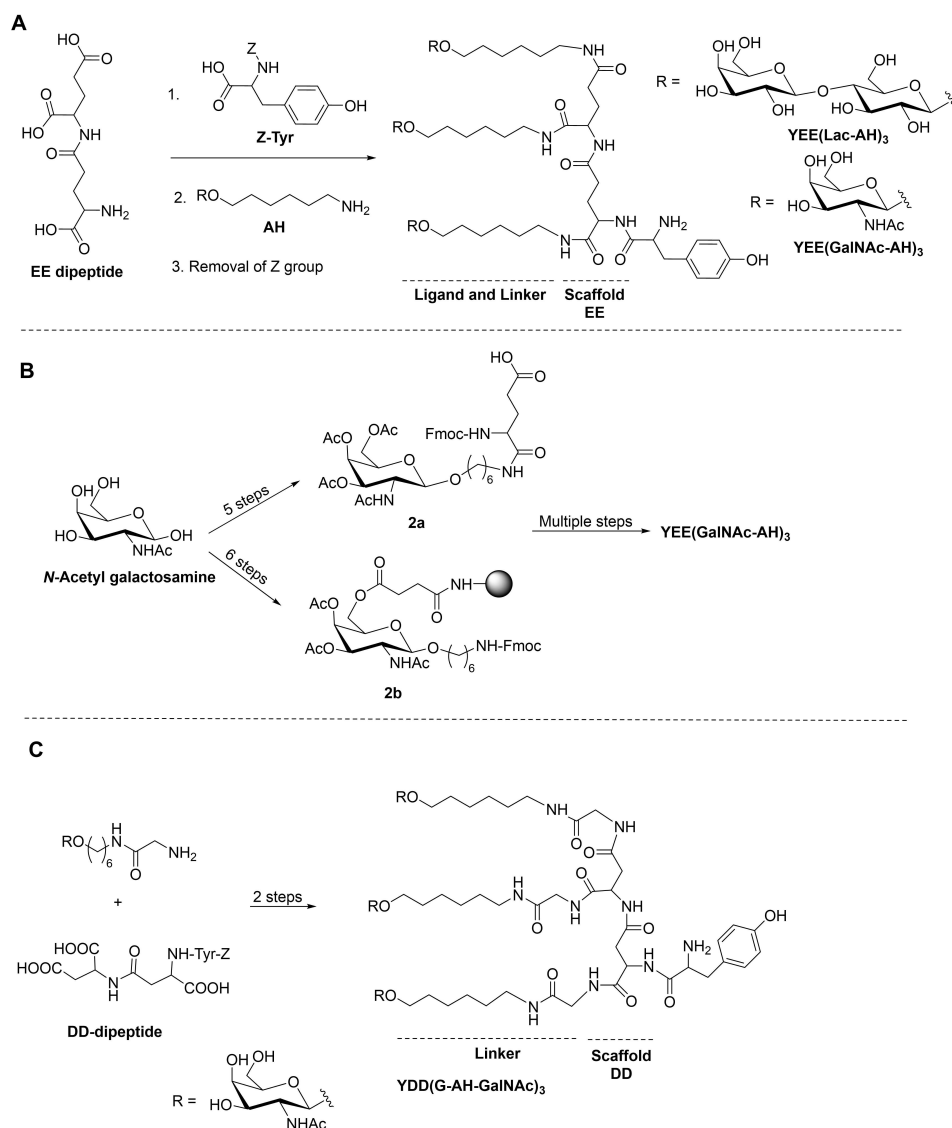
EurJOC
European Journal of Organic Chemistry

Review
doi.org/10.1002/ejoc.202201360

Chemistry
Europe
European Chemical
Societies Publishing

Figure 2. Peptide scaffold based trivalent galactosides. (A) Lactose based glycotripod; (B) Galactosamine based glycotripod; (C) Galactosamine glycine based glycotripods.

well recognized by ASGPR receptors when the vicinal galactose units have proper spacing.

In 1994, Biessen et al.[28] synthesized trivalent galactoside with 20 Å tetraethyleneglycol spacer between the galactose unit and main scaffold which was named TG(20 Å). The spacing of 20 Å between the galactose and main scaffold made the galactose units more flexible than the TG(4 Å). Further this trivalent galactoside was conjugated with cholesterol to afford TG(20 Å)C (Figure 4A). The inhibition constant of TG(20 Å)C was 200 ± 76 nM and it targeted low density lipoprotein (LDL) to parenchymal cells and thus facilitated the removal of LDL derived cholesterol from the body. A single intravenous injection of TG(20 Å)C in rats led to a reduction in the serum cholesterol concentration.

The TG(20 Å)C was the most potent compound for lowering the cholesterol level but the rapid exchange of glycolipid occurred due to the high hydrophilicity of glycolipid and hence

only 20% of liver uptake was achieved. Furthermore, acid labile acetal linkage in TG(20 Å)C reduces the chemical stability of glycolipid. To address these problems of acetal linkage and high hydrophilicity, Sliedregt et al.[29] synthesized the novel amphiphilic glycolipid in which acetal linkage was replaced with a more stable ether linkage (Figure 4B). Hence, ether linked glycolipids were synthesized by using pentanoic acid conjugated galactoside which was earlier used in the solid phase synthesis. Lipids were conjugated to trivalent galactosides in multiple steps to obtain the desired glycolipids **4a–4e** (Figure 4B). Trivalent galactoside without lipid unit shows strong binding affinity with ASGPR (93 nM) which is similar to TG(20 Å) (200 nM). All glycolipids form small micelles of 8–10 nm in size which can be distinguished from the large size liposomes (27 ± 0.3 nm). These glycolipids can associate with liposomes and have superiority over the earlier synthesized glycolipid in terms of chemical stability, accessibility, and high affinity for ASGPR. In
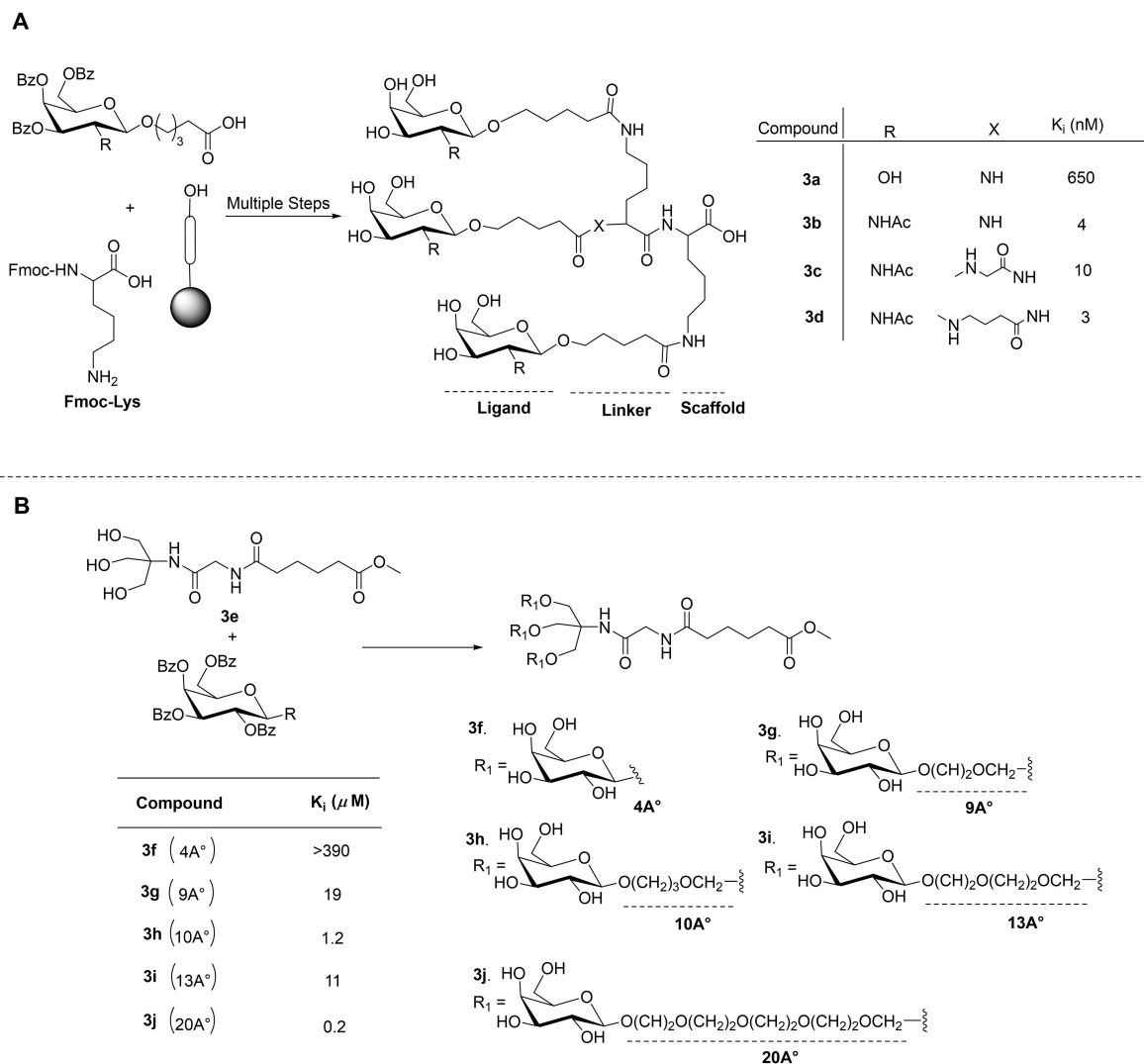
EurJOC
European Journal of Organic Chemistry

Review
doi.org/10.1002/ejoc.202201360

Chemistry Europe
European Chemical Societies Publishing

Figure 3. (A) Lysyl-lysine scaffold based galactosides; (B) TRIS scaffold based galactosides.

2007, Hai and coworkers[30] synthesized cholesterol conjugated trivalent thiogalactoside (**4h**). The tetra-antennary mesylated dendron (**4f**) was used for the attachment of thiogalactose and cholesterol. The cholesterol unit was linked to the main scaffold using a commercially available diethylene glycol unit (**4g**, Figure 4C).

Although the above glycolipids (**4a**–**4e**) showed stable interactions with lipidic particles in the blood and effectively target the liposomes to the ASGPR of hepatocytes, high glycolipid surface density led to the elimination of liposomes by galactose particle receptor and hence glycolipid redirected LDL to the Kupffer cells. To address this problem, in 2004, Rensen et al.[31] synthesized the *N*-acetylgalactosamine terminated glycolipid with high affinity and specificity for ASGPR. Mainly two changes were done in the synthesis of amphiphilic glycolipid. The tyrosine moiety was introduced in the glycolipid to allow trace labeling which enables the kinetic studies in vivo. In addition to this, the galactose moiety was replaced with *N*-acetyl galactosamine (Figure 5). These changes in glycolipids

led to 50 fold increase in the binding affinity towards ASGPR. The synthesized glycolipid **5** can bind the plasma lipoproteins which induce the uptake of LDL and HDL by hepatocytes. Injection of this glycolipid resulted in a prolonged lowering of cholesterol level in the mouse model of hypercholesterolemia.

After optimization of tripodal glycoconjugate with the best affinity for ASGPR, drug conjugates of tripodal glycoconjugates were synthesized. In 2018, Petrov et al.[32] synthesized the paclitaxel (PTX) conjugated trivalent *N*-acetyl galactosamine conjugates using click chemistry. The azide part of trivalent *N*-acetyl galactosamine was coupled with the alkyne part of PTX to obtain the desired trivalent glycoconjugate **tri-GalNAc-paclitaxel** (Figure 6A). In the biological evaluation with ASGPR expressing HepG2 cell line, it was revealed that the monovalent conjugate of PTX shows better cytotoxic potency ($CC_{50} = 0.092$ μmol) as compared to corresponding trivalent conjugate ($CC_{50} = 0.11$ μmol). Targeted delivery of taxanes for treating hepatocellular carcinoma using a high molecular weight delivery system is a well-explored system. However, most of
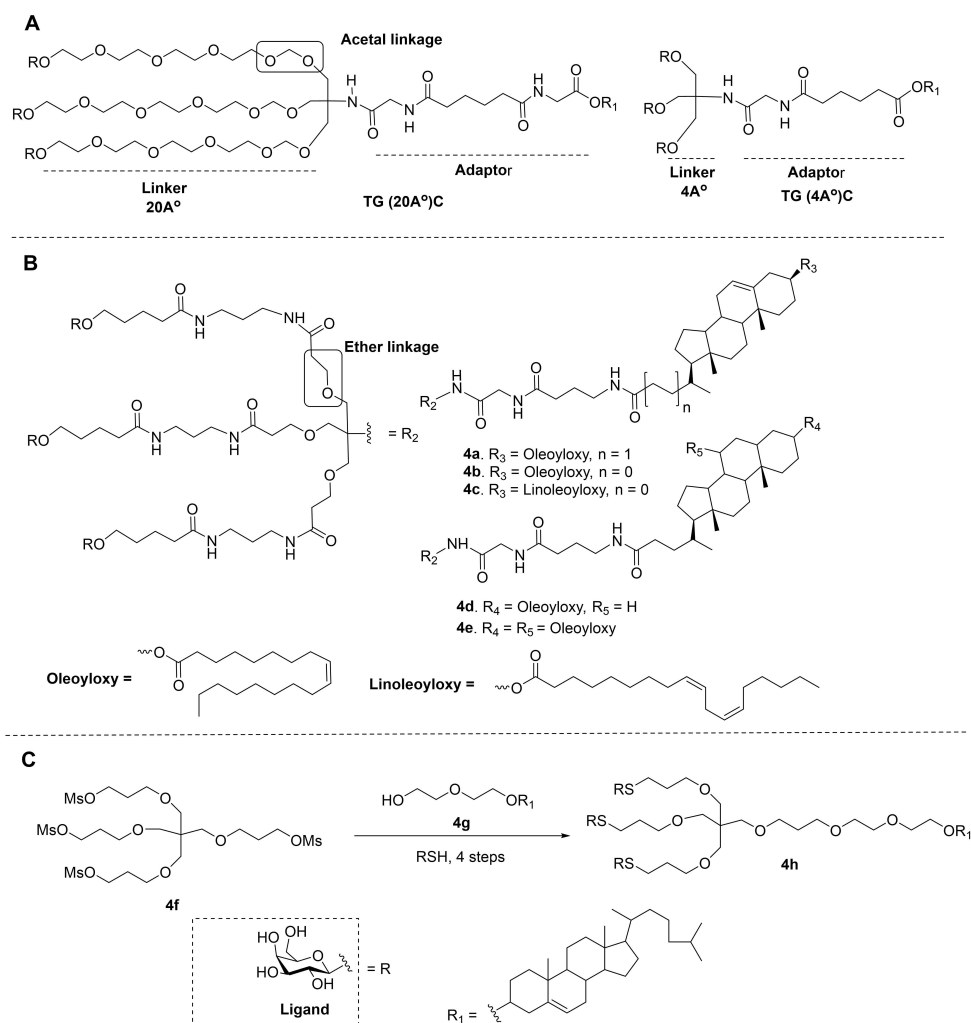
EurJOC
European Journal of Organic Chemistry

Review
doi.org/10.1002/ejoc.202201360

**Chemistry
Europe**
European Chemical
Societies Publishing

Figure 4. (A) TRIS scaffold based trivalent galactolipids; (B) Tris scaffold based ether linkage containing galactolipids; (C) Cholesterol conjugated trivalent thiogalactoside.
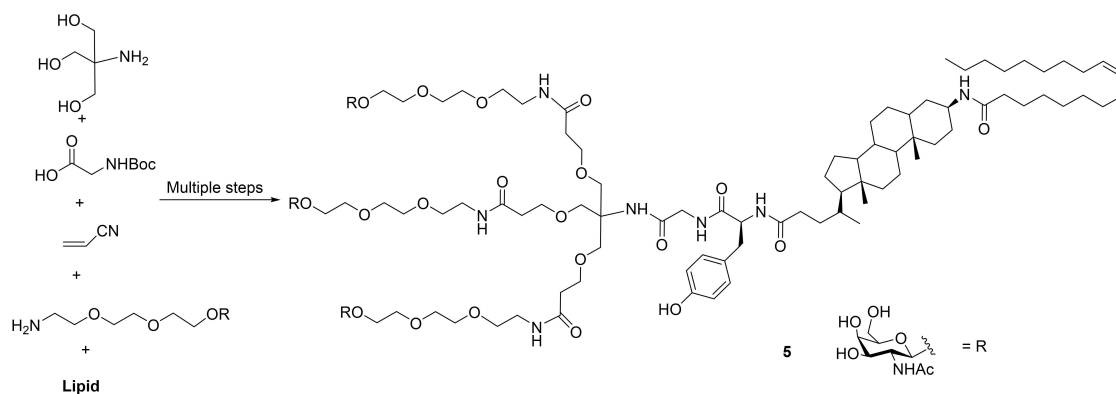

Figure 5. Tris scaffold based glycolipids.

these systems rely upon passive transport. In 2021, Petrov et al.[33] synthesized the docetaxel (DTX) delivery system based on conjugation with trivalent N-acetylgalactosamine glycoconjugates **tri-GalNAc-docetaxel** (Figure 6A). The synthesized gly-

coconjugates of docetaxel have better water solubility (21–75 fold increase) than the parental docetaxel and have binding affinity in the nanomolar range for ASGPR. The docetaxel-based glycoconjugates facilitate the enhanced generation of ROS in
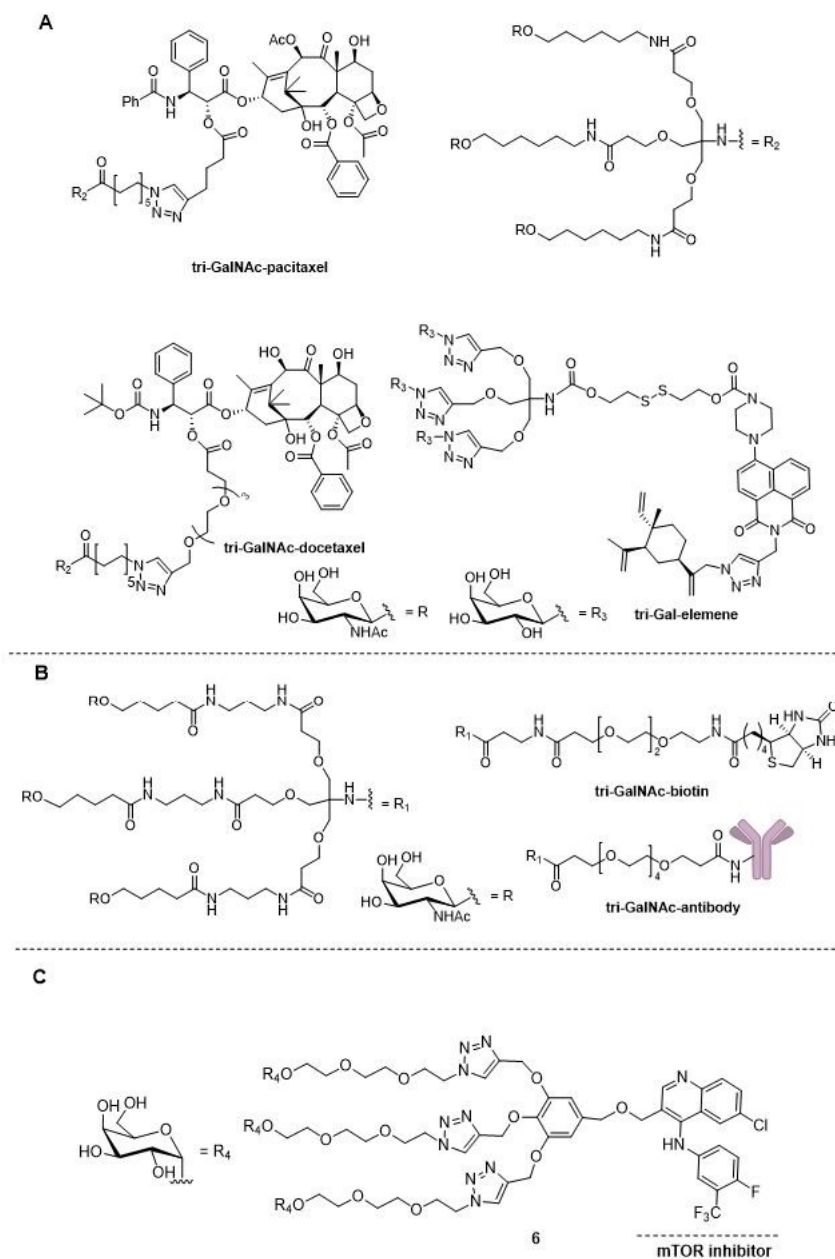
EurJOC
European Journal of Organic Chemistry

Review
doi.org/10.1002/ejoc.202201360

Chemistry
Europe
European Chemical
Societies Publishing

Figure 6. Drug loaded trivalent galactosides.

HepG2 cells and thus indicate the potential for targeted treatment of hepatocellular carcinoma.

In 2021, Wang and coworkers[34] synthesized hepatocyte targeting β-elemene based prodrug using tridentate conjugated galactoside (Figure 6A). The synthesized prodrug **tri-Gal-elemene** shows good anticancer activity and low cytotoxic effect. It was demonstrated that prodrug could be released in presence of GSH (mimic condition of tumor cell) by breaking the disulfide bond. The prodrug is designed with the targeting ligand with a reductant-responsive linker which is activated by the tumor cells, reducing the side effect of the drug. The hepatocyte targeting capacity of prodrug **tri-Gal-elemene** and its parent drug was evaluated in vivo in mice. The **tri-Gal-**

elemene prodrug selectively recognizes liver tissues through ASGPR present on the hepatocyte membrane and showed the highest distribution in the liver. In 2021, Tang and coworkers[35] synthesized the triantennary *N*-acetylgalactosamine conjugates for the targeted degradation of extracellular proteins by exploring the potential of ASGPR. Biotin and antibodies were conjugated to trivalent *N*-acetylgalactosamine conjugates to develop the new class of degraders. The trivalent *N*-acetyl-galactosamine-biotin small molecule and antibody labeled trivalent *N*-acetylgalactosamine have been explored for delivering the extracellular protein targets into the lysosome for degradation (Figure 6B). In 2021, Dutta and coworkers[36] synthesized the quinoline based trivalent galactose conjugate

EurJOC
European Journal of Organic Chemistry

Review
doi.org/10.1002/ejoc.202201360

Chemistry
Europe
European Chemical
Societies Publishing

6. The quinolone moiety preferentially inhibits the mTOR (mammalian target of rapamycin) pathway and hence decreases the lipid accumulation in the cultured hepatocytes. The ethylene glycol based linker was used for connecting galactose with the main scaffold (Figure 6C). The synthesized trivalent galactose conjugate 6 shows a 17-fold binding affinity with the isolated ASGPR-H1-CRD protein receptor (K_d 54 μM) compared to the isolated galactose (K_d 900 μM). From the ITC studies, it was evident that live hepatocytes carrying ASGPR interact with galactose conjugate whereas no significant thermal response was observed with non-ASGPR Chang cells. The galactose conjugate 6 does not show significant mTOR inhibition at micromolar concentration. The less mTOR inhibition of trivalent glycoconjugate may be due to the lower potency of the acyclic quinolone core attached to the galactoconjugate 6.

To test the selective uptake of tripodal glycoconjugates by hepatic cells, the labeling of tripodal glycoconjugate with the fluorescent molecule is required for fluorescence microscopy and flow cytometry study. In 2008, Ernst and coworkers,[37] synthesized the fluorescent trivalent glycoconjugates (7a–7c)

having terminal β-galactose and N-acetylgalactosamine units to bind with ASGPR and tested them on human liver cells. The Tris scaffold and Alexa Fluor® 488 as a fluorescent probe were used in the synthesis of trivalent glycoconjugates (Figure 7A). Using fluorescence microscopy and flow cytometry, it was shown that fluorescent trivalent glycoconjugates 7a and 7b are selectively taken up by ASGPR and negligible uptake of glycoconjugate (7c) was observed on HepG2 cells derived from human parenchymal liver cells. The negligible uptake of fluorescent glycoconjugate (7c) was mainly due to insufficient spacer length. This result of fluorescent glycoconjugate (7c) further confirms the general assumption that there should be an optimal distance between the sugar molecules for better binding with ASGPR. It was demonstrated that glycoconjugate with terminal N-acetylgalatosamine has the potential for targeted delivery of therapeutic agents to the liver.

Maklakova et al.[38] synthesized hydrophilic fluorescent dye conjugated trivalent glycosides (7d–7f). The water soluble sulfo-Cy5 dye was used for conjugation with glycoside ligand (Figure 7B). The tracing of fluorescent glycoconjugates was

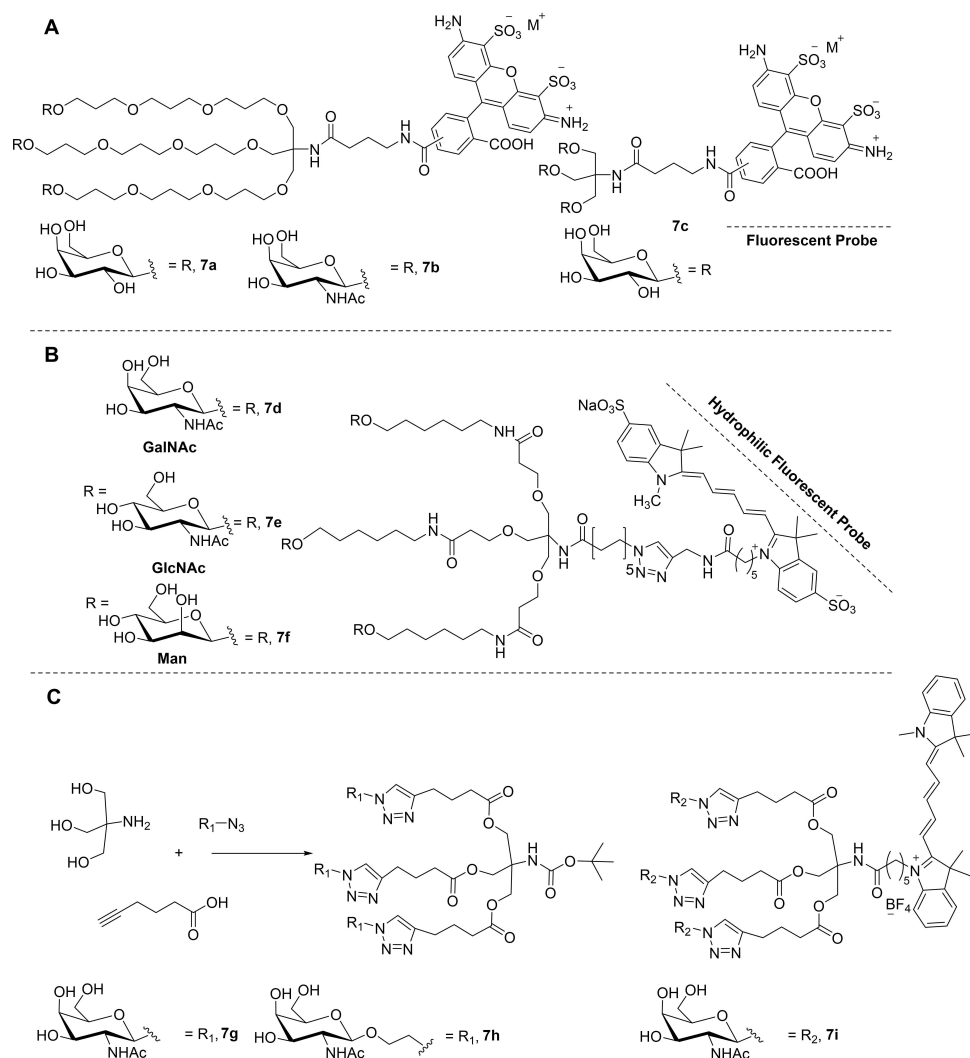**Figure 7.** Fluorescent probe based trivalent glycosides.

EurJOC
European Journal of Organic Chemistry

Review
doi.org/10.1002/ejoc.202201360

Chemistry Europe
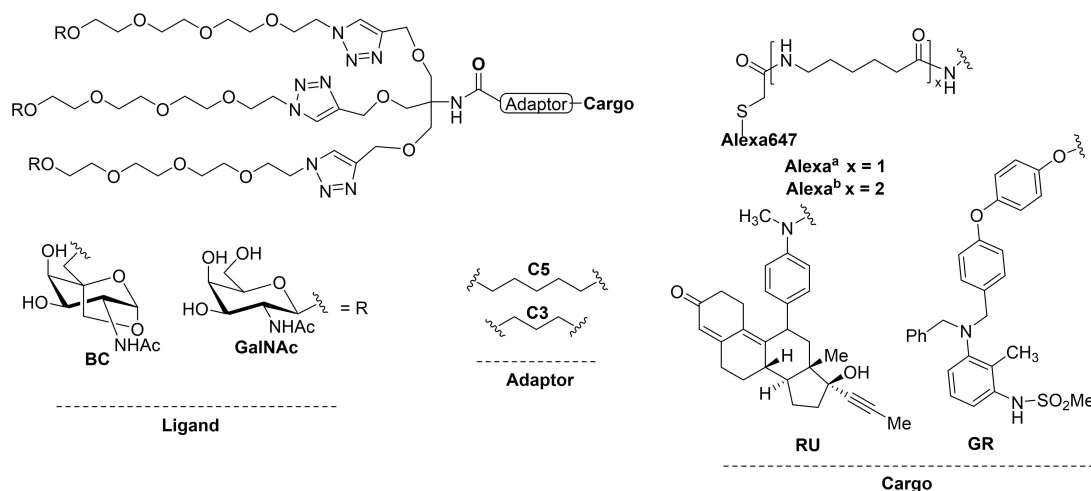European Chemical Societies Publishing

Figure 8. Fluorescent probe based trivalent galactoside.

done with intravital microscopy in real time. Among the three fluorescent glycoconjugates (**7d**–**7f**), GalNAc conjugate (**7d**) facilitated rapid and effective penetration of fluorophore into hepatocytes. On the other hand, fluorescent GluNAc (**7e**) and Man (**7f**) conjugates were unable to enter the parenchymal liver cells and accumulated in the liver sinusoidal endothelial cells. In 2020, Reshitko et al.[39] introduced the new trivalent N-acetyl-galactosamine conjugates (**7g**–**7i**) using a TRIS scaffold (Figure 7C). The triazolyl glycoconjugates **7g** and **7h** showed a binding affinity for ASGPR with K_d values 0.98 nM and 2.75 nM, respectively. Cy5 conjugated trivalent glycoconjugate (**7i**) specifically accumulated in the HepG2 cells in comparison to the PC3 cell line.

In 2017, Mascitti and coworkers[40] introduced a bicyclic bridged ketal as a ligand for ASGPR. The synthesized trivalent derivative is referred to as "Cargo-Adaptor-Ligand" like Alexa[a]-C3-(BC)$_3$ where Alexa[a] is cargo, C3 is propyl chain adaptor and BC is bicyclic bridged ligand (Figure 8). The trivalent conjugates Alexa[a]-C3-(BC)$_3$ and GR–C3-(BC)$_3$ showed binding affinity of 30 ± 5 pM and 71 ± 30 pM. The trivalent Alexa[b]-C5-(BC)$_3$ glyco-conjugate mediated predominant delivery to hepatocytes as compared to Kupffer cells in vivo. The results of biodistribution of Alexa647-labelled trivalent conjugate showed selective hepatocyte targeting and prolonged retention as compared to similar trivalent GalNAc. It was observed that the bicyclic derivate of GalNAc was superior to parent GalNAc in rate and extent of cellular uptake in vitro.

Patients with Wilson's disease have a lack of protein that pump out the copper ions from the hepatocytes and suffer from copper overload. In 2012, Delangle and coworkers[41] have devised trivalent N-acetylgalactosamine conjugates (**9a**–**9c**) which have a dual capacity to bind with Cu(I) and target hepatocytes. The binding motif was coupled with two cysteine units because Cu(I) has an affinity for the soft ligand like cysteine (Figure 9). Due to the S–S bond in the N-acetylgalac-tosamine conjugate, it can be cleaved in the reducing intra-cellular environment and hence release the ligand for Cu(I) in
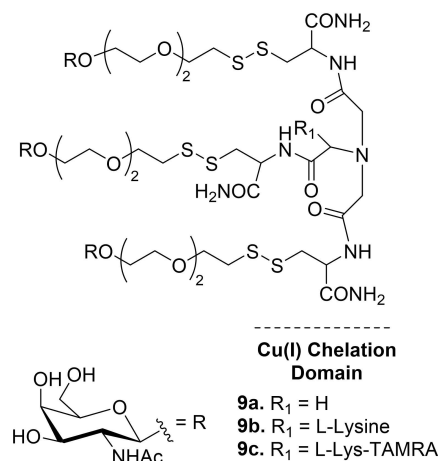

Figure 9. Chelation domain based trivalent galactosides.

the intracellular environment. The distance between each β-N-acetylgalactosamine moiety of glycotripods was kept 20 Å apart using an ethylene glycol spacer. The fluorescent analog 1-TAMRA having a carboxytetramethylrhodamine was also syn-thesized to visualize the uptake of glycotripod inside the hepatocytes.

Gene silencing techniques have been widely explored to treat various diseases including different cancers, viral infec-tions, and Parkinson's diseases. The gene silencing is done by short interfering RNA (siRNA), an antisense oligonucleotide (ASO), and peptide nucleic acid (PNA). Although all these nucleic acids have a high potential to treat these diseases, there are many challenges to their successful delivery to the target organs. Tris-GalNAc is the widely used glycoconjugate as a vehicle to deliver the cargo in the liver. Tris-GalNAc has a high tendency to bind with asialoglycoprotein receptors which are abundantly present on the surface of hepatocytes and result in rapid endocytosis. Therefore, Tris-GalNAc-Nucleic acid conju-gates have attracted attention for delivering nucleic acid into

EurJOC
European Journal of Organic Chemistry

Review
doi.org/10.1002/ejoc.202201360

Chemistry
Europe
European Chemical
Societies Publishing

the liver. The receptor binding is mediated by Ca^{2+} and is sensitive to pH. The nucleic acid can be delivered in the hepatocytes due to a pH drop in the hepatocytes and ASGPR got attained its original position on the surface of hepatocytes (Figure 10). Many GalNAc-siRNA conjugates are underway in clinical trials to treat wide variety of diseases.

In 2015, Ostergaard et al.[42] described a solution phase synthesis of 5′-hexylamino modified ASO conjugate trivalent *N*-acetylgalactosamine **11a**. The conjugation reaction of modified ASO and trivalent *N*-acetylgalactosamine was performed in a multigram scale. The trivalent *N*-acetylgalactosamine was conjugated to the 5′-end of ASO. It was found that the transfer of trivalent *N*-acetylgalactosamine from the 3′-end of ASO to the 5′-end led to an increase in the potency of ASO by two folds in cell culture and 1.5 folds in animals. The drug was extracted from mice's liver after 72 h of post injection to further investigate metabolic properties of 3′-GalNAc modified ASO and 5′-GalNAc modified ASO. The study of extracted mice liver showed that the 5′-GalNAc modified ASO was fully metabolized to release the parent ASO but in 3′-GalNAc modified ASO incomplete metabolization was found after 72 h. In 2016, Prakash et al. synthesized antisense oligonucleotide (ASO) based *N*-acetylgalactosamine conjugates to enhance the potency of ASO to the hepatocytes.[43] Six distinct branched or amino acid scaffolds were synthesized and coupled with ASO using simplified solution phase or phosphoramidite based methods. The detailed structure-activity relationship was studied for enhancing the potential of ASO by changing the length and hydrophobicity of the linker attaching GalNAc to the scaffold. Among these various synthesized ASO-glycoconjugates, the tris-hexylamine GalNAc cluster (THA-GN3) (**11b**, Figure 11) was identified as the best glycoconjugate for synthesis in terms of cost and simplicity. The THA-GN3-ASO conjugate targeting apolipoprotein was shown to be 30-fold more potent than the parent ASO in humans. The measurement of changes in white blood cell count (WBC) showed no

significant inflammation in animals treated with THA-GN3-ASO as compared to parent ASO. Seth and coworkers[44] synthesized the ASO-GalNAc conjugate **11c** from the linker of eight carbons using solid support synthesis. Conjugation of trivalent GalNAc improves the potency of ASO by 10-fold in mouse models due to the direct delivery of ASO in hepatocytes. Further, 60-fold potency was improved for the next generation as compared to parent second-generation 5-10-5 MOE (2′-*O*-methoxyethyl RNA) ASO (**11c**, Figure 11). The mice were injected with ASO-GalNAc conjugate to observe its metabolism. After 72 h post injection, the extracted liver showed that no portion of GalNac was attached with ASO which indicates the release of free ASO in the liver. Ganesh and coworkers[45] synthesized the peptide nucleic acid (PNA) conjugated trivalent *N*-acetylgalactosamine via solid phase synthesis. The PNA was conjugated with *N*-acetylgalactosamine in two different ways: (1) a trivalent branched *N*-acetylgalactosamine was linked at the *N*-terminus of the PNA through a spacer chain **11d** and (2) the three monovalent *N*-acetylgalactosamine units were conjugated sequentially at C_γ of the backbone on the *N*-terminal of PNA residue **11e**. Furthermore, for cell permeability studies, carboxy-fluorescein was labeled at the *N*-acetylgalactosamine conjugate PNA **11f**. It was observed that the internalization of sequential *N*-acetylgalactosamine conjugates PNA is 13-fold more efficient than the branched *N*-acetylgalactosamine conjugates PNA.

In 2014, Manoharan and coworkers[46] designed the synthesis of siRNA based trivalent glycoconjugates **11g** using solid phase oligonucleotide synthesis. Already synthesized trivalent *N*-acetylgalatosamine conjugate was functionalized for the covalent conjugation of siRNAs. A *trans*-4-hydroxyprolinol moiety was introduced to enable site specific conjugation of ligand to any position of oligonucleotide during the solid phase synthesis. The robust uptake of trivalent GalNAc-siRNA was observed as compared to the unconjugated siRNA in the freshly removed mouse hepatocytes. These conjugates inhibit targeted gene expression in mice with a single dose ED_{50} value of
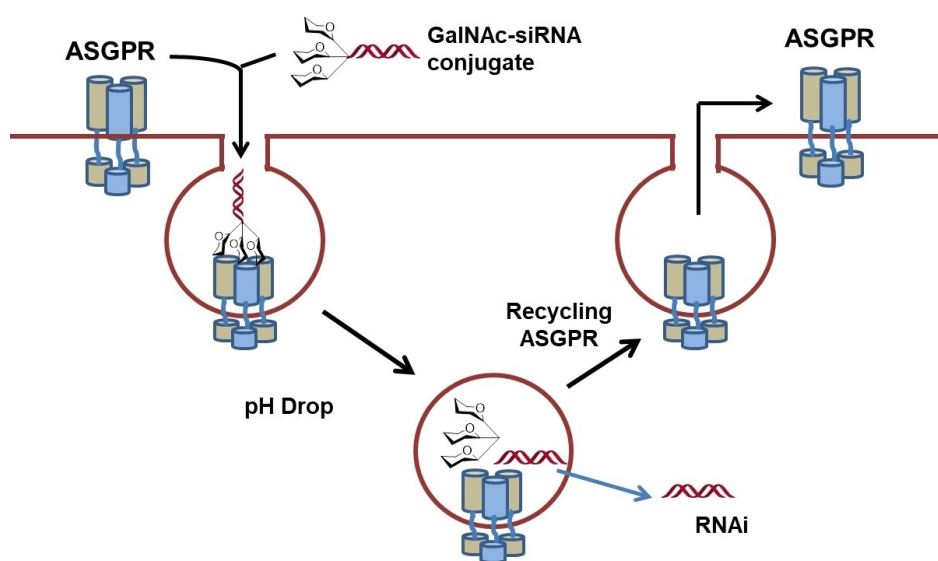

Figure 10. Delivery of GalNAc-siRNA conjugate in hepatocytes.

EurJOC
European Journal of Organic Chemistry

Review
doi.org/10.1002/ejoc.202201360

Chemistry
Europe
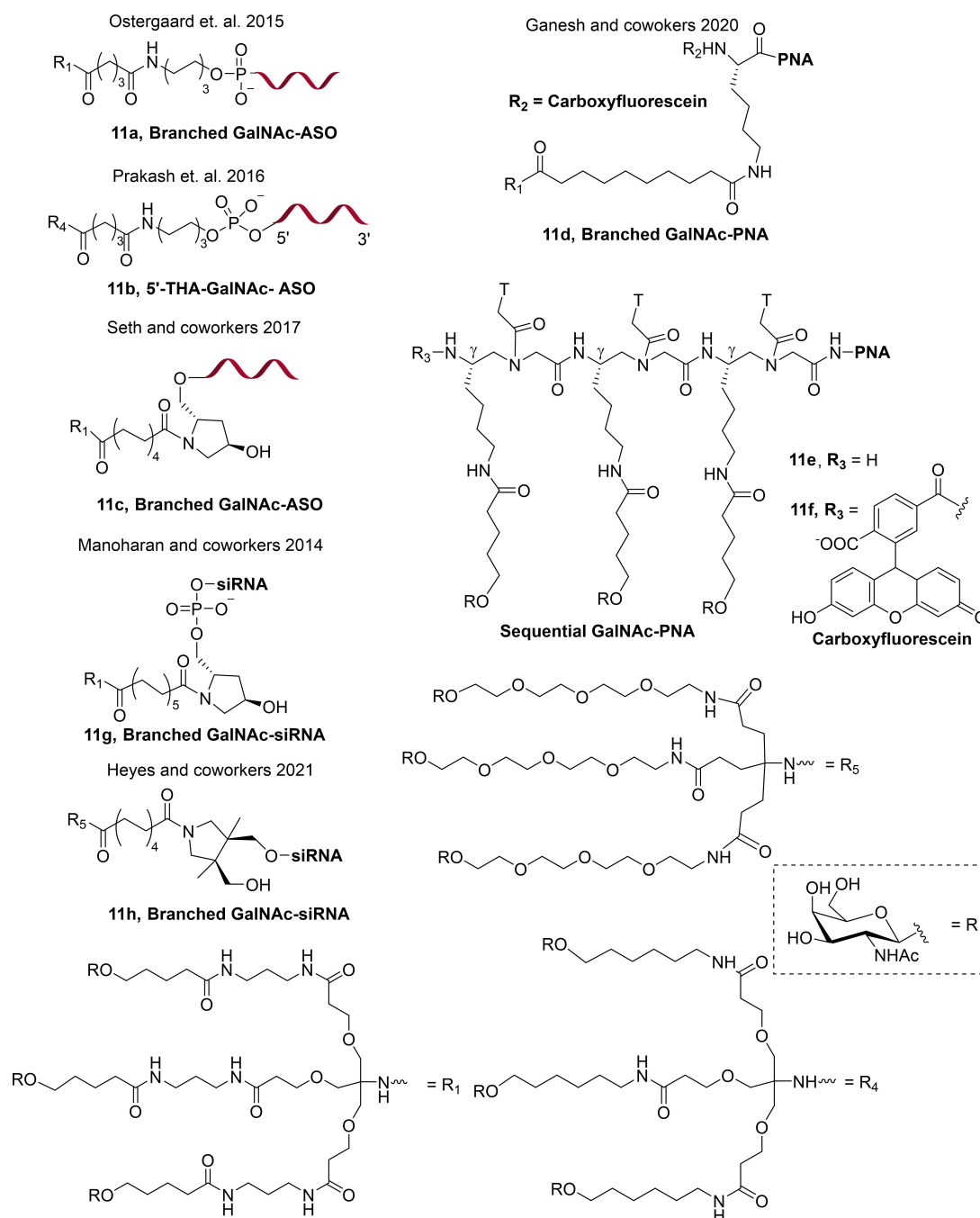European Chemical
Societies Publishing

Figure 11. Nucleic acid conjugated trivalent galactosides.

1 mg/kg. In 2021, Heyes and coworkers[47] explored the effect of linkers on the potency of siRNA. It was shown that there is small difference in biological performance between bivalent, trivalent, and tetravalent glycosides conjugates but the other factors are also affecting the biological performance more significantly (**11 h**, Figure 11).

In 2017, Seth and coworkers[48] synthesized ASO-conjugated *N*-acetylgalactosamine for the enhanced delivery of modified ASO in the hepatic cells (Figure 12A). The monovalent *N*-acetylgalactosamine-ASO conjugate showed a 10-fold reduced

affinity as compared to the trivalent acetylgalactosamine-ASO conjugate. The results of this paper also demonstrated that the backbone charge and chemical composition of oligonucleotide assist in the binding and internalization of highly polar anionic single stranded ASO into hepatic cells. In 2015, Rajeev et al.[49] simplify the design of siRNA-GalNAc conjugate by synthesizing a non-nucleosidic monovalent GalNAc unit which is further converted into trivalent GalNAc in a sequential manner (Figure 12B). The 3′-end of siRNA was conjugated by solid phase oligonucleotide synthesis. The uptake efficiency of sequential

EurJOC
European Journal of Organic Chemistry

Review
doi.org/10.1002/ejoc.202201360

Chemistry Europe
European Chemical Societies Publishing

glycoconjugates was comparable to the parent triantennary GalNAc for ASGPR.

Derdau and coworkers[50] developed a bifunctional probe to monitor the expression of ASGPR for the detection of non-alcoholic steatohepatitis (NASH) progression. The bifunctional GN (GalNAc-NASH) probe was synthesized by conjugation of trivalent GalNAc with Gallium (^{68}Ga) labeled dodecane tetra-acetic acid (DOTA) to allow positron emission tomography (PET) imaging and/or with hexamethine cyanine dye (Cy5.5) to allow infrared optical imaging. The radioisotope ^{68}Ga has strong chelation with dodecane tetraacetic acid. The Cy5.5 labeled GN probes were incubated with HepG2 human hepatocytes and localization and intensity monitored by confocal microscopy. It has been observed that the intensity of the signal is increasing with time without affecting the cell viability. The radioactive GN (GalNAc) probes show stability in plasma and were used in in vivo studies in rodents. The radiolabelled GN probes were used for monitoring the progression of NASH and fibrosis over a long period beyond the need to sacrifice the animal (Figure 13).

3. Hemagglutinin

Hemagglutinin (HA) is a receptor binding membrane glycoprotein that is found on the surface of the *Paramyxoviridae* and *Orthomyxoviridae* family viruses. The term "hemagglutinin" comes from the Greek word: hema, which means "blood" and the Latin root: agglutinatus, which means "glued or clump
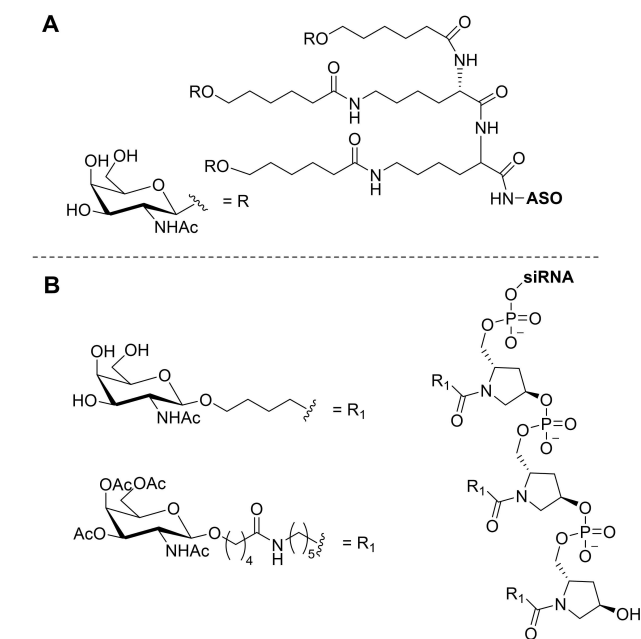
Figure 12. (A) ASO based trivalent glycoconjugate; (B) siRNA based trivalent glycoconjugate.

together" and hence represents the ability of the protein to cause agglutination of red blood cells. The HA glycoprotein is responsible for the binding of the viruses such as influenza virus
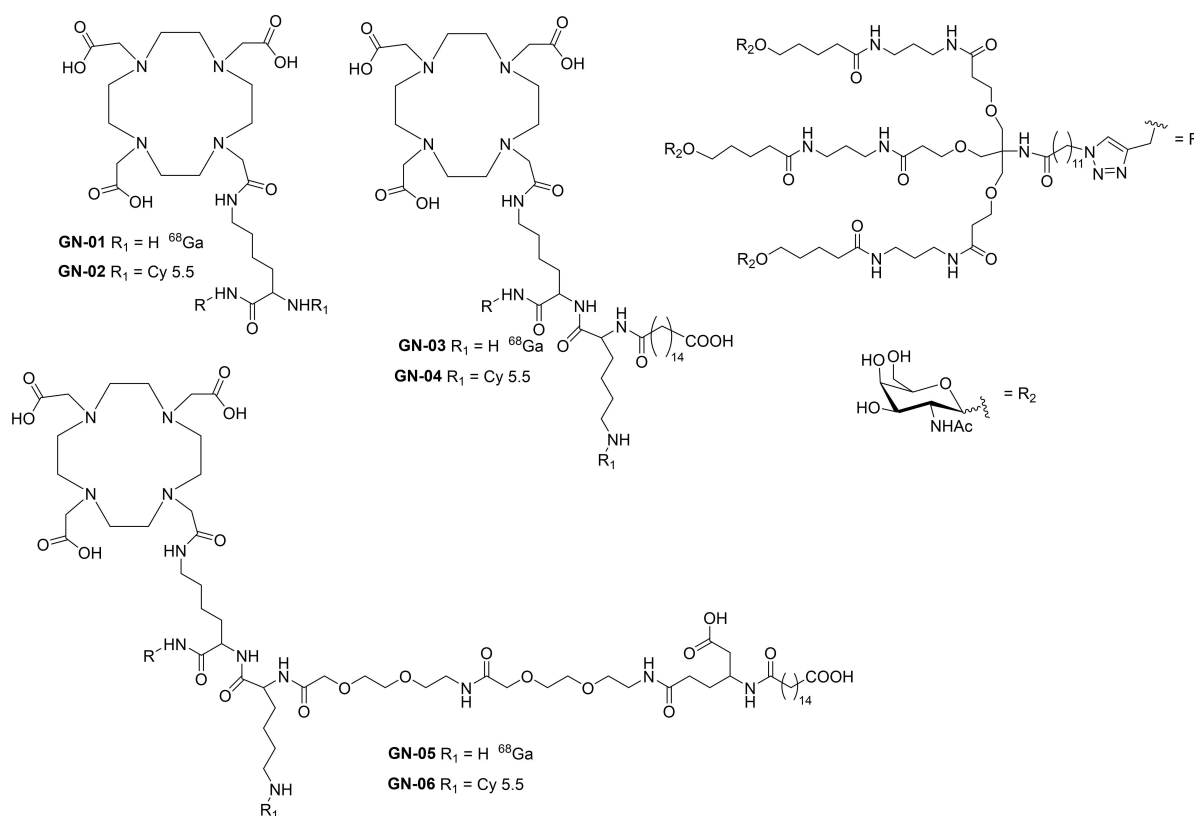
Figure 13. Radioactive labeled trivalent galactosides.

EurJOC
European Journal of Organic Chemistry

Review
doi.org/10.1002/ejoc.202201360

Chemistry Europe
European Chemical Societies Publishing

to the host cell via various sialic acid (SA) receptors expressed on the cell plasma membrane. The cell membrane then engulfs the viral particle through endocytosis and infection is triggered. Structurally, HA is a highly abundant cylindrical-shaped homo-trimeric protein with an approximate height of 13.5 nm from the virus surface.[51] HA-trimer (HA_3), comprised of three identical monomers, is densely packed on the viral envelope and two adjacent HA_3 are 10–12 nm centrally apart from each other. The crystal structure of the HA_3 from a human H3 N2 strain (PDB ID: 1hgg) revealed that the planar distance between two SA-binding sites on a single HA_3 is around 4–6 nm (Figure 14) and a typical spherical influenza A virus of diameter 120 nm carries around 400–500 HA_3 units.[52,53]

Since each monomer of the HA_3 has a receptor binding site (RBS) for SA, therefore, scaffolds decorated with SA moieties thus competing with cell surface virus receptors have been favorably implemented in several studies to inhibit the activity of HA and thus influenza virus replication.[54–59] Considering the trimeric spatial organization of HA, a high affinity tripodal/trivalent ligand could be designed by choosing an appropriate trivalent core and a spacer to bring the three HA-binding moieties in the right geometry that matches the RBSs of HA_3. Several research studies have demonstrated the significance of 1,3,5-trisubstituted benzene scaffold for C_3 symmetric presentation of glycosidic ligands to construct trivalent/tripodal glyco-sides for lectin binding and other biological applications.[60–62]

Meyer and coworkers employed a trimesic acid core to construct a trivalent SA ligand as a HA binding scaffold (Figure 15).[63] For the synthesis of trivalent compounds, compounds **15a** and **15b**, which were synthesized in several steps from trimesic acid and sialic acid, respectively, were reacted together in the presence of coupling reagent TBTU under the basic condition in DMF to produce compound **15c**. The basic hydrolysis of trivalent sialoside **15c** using NaOMe and NaOH in two steps finally produced compound **15d**. The lengths of the peptide and alkyl chain were varied to assess their binding energy and subsequently an energetically favored optimized compound **15e** was synthesized. In the optimized compound, the anomeric center of the SA is spaced by 42 bonds which bridged the distance of 3 nm from the aromatic core and ultimately allowed the simultaneous binding of all three SA to the HA_3. A binding constant of 446 nM determined by surface plasmon resonance (SPR) was obtained with HA_3 of influenza A virus type H5 which is 4000-fold higher as compared to monovalent compound 2-*O*-methyl-α-D-*N*-acetylneuraminic acid.

Based on earlier studies demonstrating the inhibition of HA_3 by trimesic acid-based tripodal glycoconjugates, tripodal fucoi-dan derivatives were synthesized using trimesic acid and found to be reasonably active in binding HA_3. Kosono et al. chemically synthesized a series of fucoidan derivatives to inhibit the activity of viral HA.[64] The docking simulation studies showed
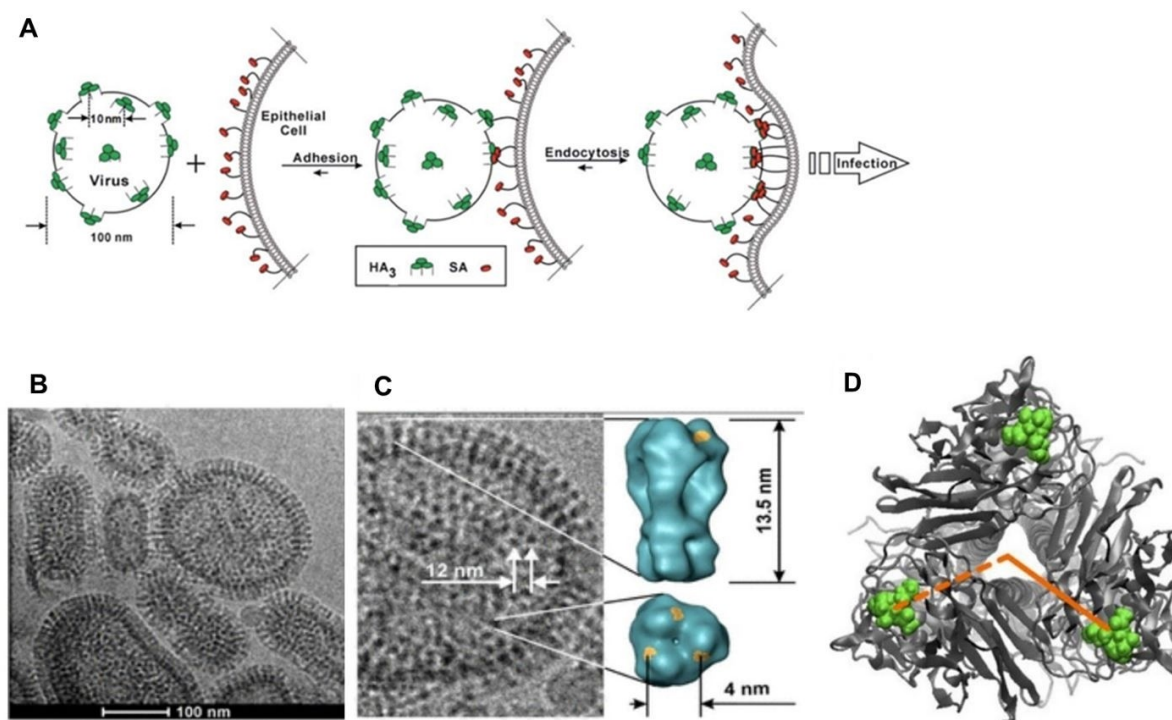

Figure 14. (A) Diagram showing the HA proteins on the surface of influenza virus and their interactions with SA residues of host cells which lead to endocytosis and infection. Reproduced from Ref. [7]. Published by the Royal Society of Chemistry under the terms of a CC BY-NC 3.0 license; (B) cryo-TEM image of influenza A virus showing the abundance of surface hemagglutinin (HA) protein. Reproduced with permission from Ref. [6]. Copyright (2016), American Chemical Society; (C) Representation of a single HA spike which has an average length of 13.5 nm from the virus surface and on the top 3 sialic acid binding pockets which are around 4 nm from each other. Reproduced with permission from Ref. [51]. Copyright (2010), Wiley-VCH; (D) Top view of HA_3-region where bound SAs are highlighted in green. Reproduced from Ref. [68]. Published by Wiley-VCH under the terms of a CC-BY-NC 4.0 license.

EurJOC
European Journal of Organic Chemistry

Review
doi.org/10.1002/ejoc.202201360

Chemistry Europe
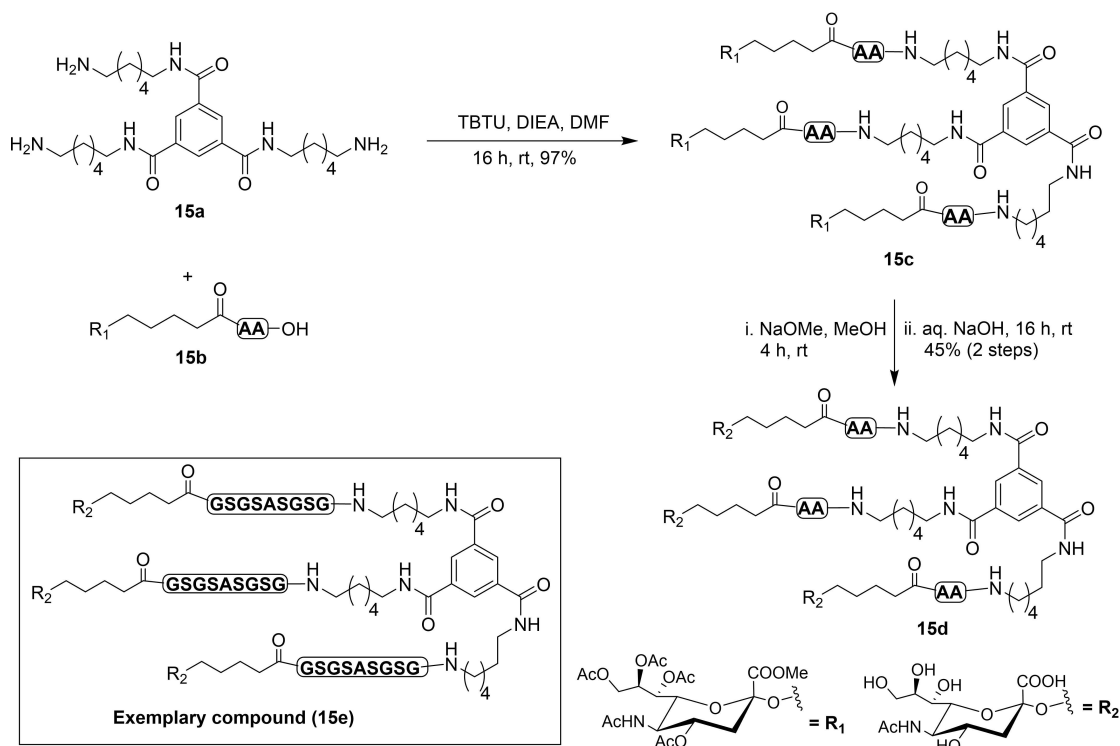European Chemical Societies Publishing

Figure 15. Key steps for the synthesis of SA-functionalized peptide-linked trivalent compounds and the structure of the most active compound.

that one of the synthesized fucoidan derivatives bound to viral HA at the same site as the native sialylated ligand with an affinity similar to that of the natural ligand. An optimized tripodal compound **16a** (Figure 16A) exhibited 65 and 70-fold higher binding activity towards H1 HA and H3 HA, respectively as compared to its monomeric analog as determined by avidin-biotin-peroxidase complex (ABC) assay. Moreover, the sulfated fucoidan moiety was found to be inert towards enzymatic hydrolysis by viral NA protein.

Recently, Lu et al. also reported on the synthesis of SA functionalized trivalent inhibitors where optimized compound showed more than a 400-fold increase in affinity against HA compared to the monovalent ligand.[65] The IAV inhibition potential of the compound was evaluated by testing against the H3-containing WU95 virus. The number of infected cells determined at 7 h post infection corresponded to the IC_{50} value in the micromolar range. Feng et al. synthesized tripodal sialyllactosides (**16b** and **16c**) using trisphenol and trisaniline core and extended the length of the spacer using triethylene glycol, glutamine, and C6 alkyl chain (Figure 16B).[66] Trisphenol and trisaniline cores were chosen as both have a relatively rigid conformation and a symmetric sp^3 carbon so that three branches spread out evenly. Glutamine residue was introduced in the spacer as a linker between the aglycon part and
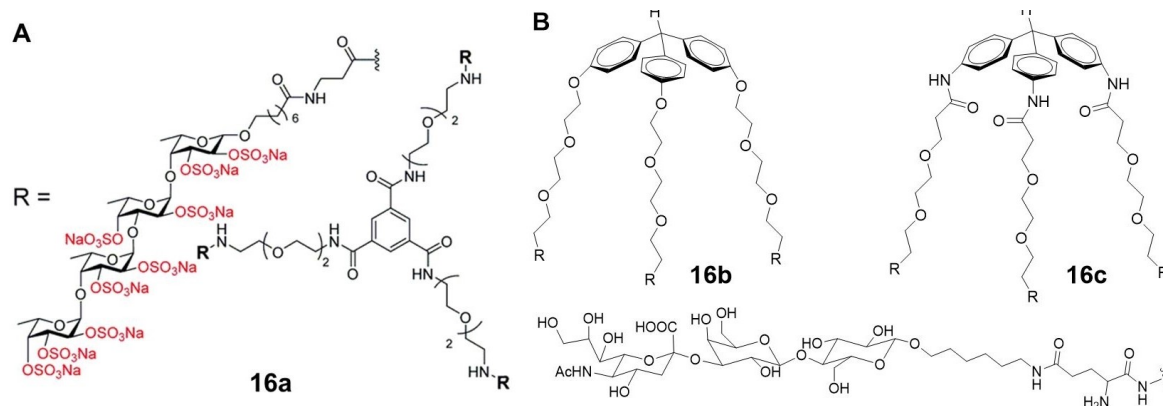

Figure 16. (A) Molecular structure of the active trimeric fucoidan compound and (B) trivalent compounds based on symmetrical trisphenol and trisaniline core.

EurJOC
European Journal of Organic Chemistry

Review
doi.org/10.1002/ejoc.202201360

Chemistry
Europe
European Chemical
Societies Publishing

sialyllactose to induce an additional interaction with the Gln189 residue of HA in addition to the interaction of sialyllactose with the HA receptor site. The modeling studies suggested that the position of the glutamine residue and the length of the linkers were appropriate and the designed tripodal compound bound efficiently with HA as per the computer simulation study but unexpectedly both the synthesized compounds did not show any HA binding activity in an inhibition assay.

In another significant contribution, authors synthesized a series of cyclic peptides (**17a**–**17c**) presenting one, two, and three sialotrisaccharides in tripodal conformation (Figure 17).[67] For the synthesis, a cyclic peptide containing glutamine (Gln) residues was coupled with 6-aminohexyl lactoside using trans-glutaminase to afford the mixture of mono-, di- and tri-substituted lactose derivatives. Sialic acid was then introduced on lactose units by using CMP-Neu5Ac in the presence of α-2,3-(N)-sialyltransferase to afford final products (**17d**–**17l**). Molecular modeling studies indicated that the maximum distance between sialic acid residues is 5–7 nm for the tripodal glycopeptides. Since the binding sites within the HA_3 are separated by 4–5 nm, all the tripodal ligands can simultaneously occupy the HA_3 binding sites. However, the hemagglutinin assay showed that biological activity is strongly determined by the amino acid sequence of the cyclic peptide, regardless of the similarity in their circular sizes. These studies demonstrated that the design of the tripodal scaffold is still challenging and there are several parameters to fine-tune the tripodal glyco-conjugate for optimum interaction with HA.

The relevance of the rigidity of the trivalent core and length of the spacer carrying the sialoside ligands was investigated by Kiran et al.[68] Compounds were synthesized by employing carboxylic acid functionalized trivalent adamantane and tris-propionic acid cores as the starting materials. Due to the different degrees of rotational freedom on the functionalizable points on the two different scaffolds, adamantane was considered to be more rigid as compared to the tris-propionic acid core. Both the rigid and flexible scaffolds were coupled with propargyl amine in the presence of carbodiimide coupling reagent to afford propargyl derivatives which were converted into azide functionality in two steps. The propargylated sialic acid was then coupled to afford desired sialic acid functionalized tripodal compounds. The authors systematically varied the spacer length on two structurally different trivalent cores to fine-tune the ligand spacing to match the binding sites on HA_3. The synthesis and molecular structures of the two representative compounds (**18d** and **18e**) are shown in Figure 18. Based on the crystal structure of the single HA_3, it was found that the projected distance between the receptor binding pockets and the HA_3 midpoint is around 2.6 nm. Moreover, the binding site was found ~0.9 nm below the top of the HA surface, which lead to an effective distance of 3.5 nm. The part of the synthesized tripod had a length of ~1.2 nm from the core to the functional group thus spacer had to bridge a distance of ~2 nm which was coved by the PEG containing 6–14 ethylene glycol units as suggested by molecular dynamic simulation studies.[69] Furthermore, the flexible tris-propionic acid core-based tripodal compound showed a binding constant in the millimolar range and the rigid adamantane core-based compound outperformed the tris-propionic acid-based compound
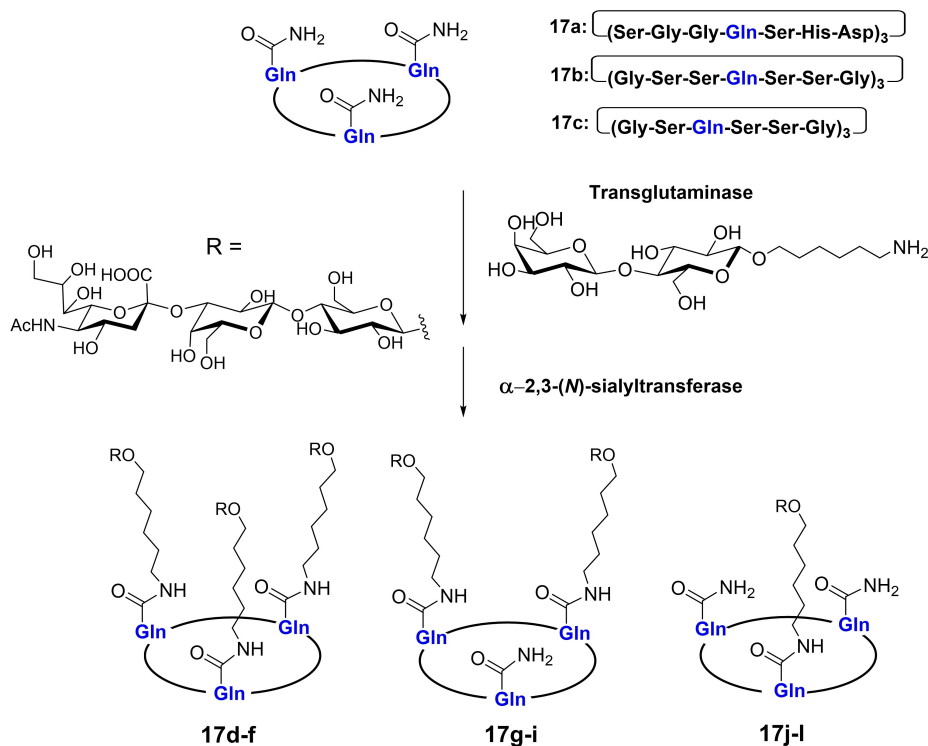

Figure 17. Enzymatic synthesis of mono-, di- and tri-valent cyclic peptide-based sialyllactosides.

EurJOC
European Journal of Organic Chemistry

Review
doi.org/10.1002/ejoc.202201360

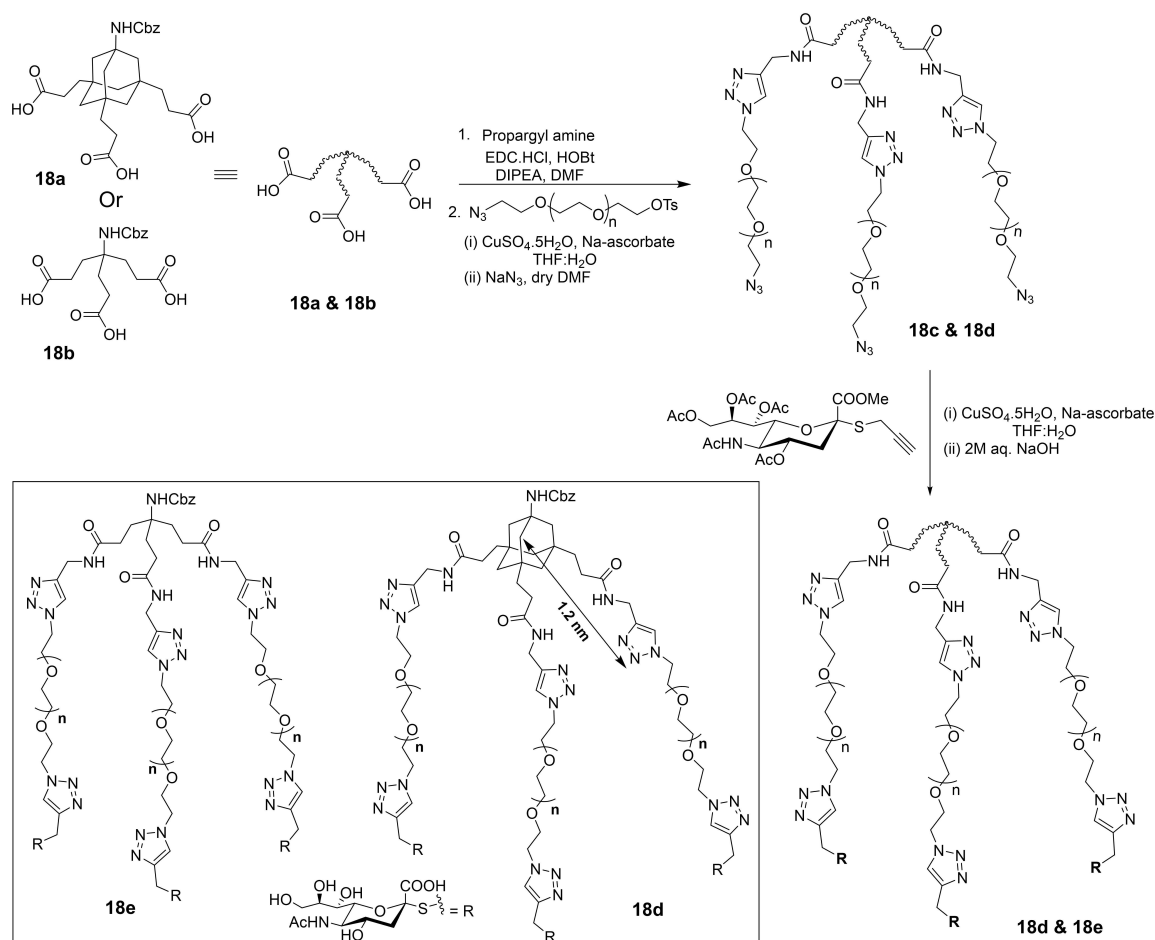**Chemistry Europe**
European Chemical
Societies Publishing

Figure 18. General synthesis of the trivalent compound and the molecular structures of representative compounds with flexible tris-propionic acid and rigid adamantane core.

with micromolar binding constant as determined by microscale thermophoresis (MST) technique.

Nagao et al. reported the topological design of sialyllactose-based star polymers for targeting HA protein (Figure 19).[70] The star structures were designed to be tripodal to allow for multiple binding to trimeric sugar-binding pockets of HA. The precise arrangement of sialyllactose units towards the binding pockets of HA was achieved by controlling the length of the arms of star polymer, the maximum interaction was found when the diameter of the polymer was comparable to the distance between the sugar binding pockets of HA. Depending upon the length of the polymeric arm, around 1.8–2.7 binding sites were accessible to bind with three arm star polymers out of total 3 binding sites, and the average inhibition constant of 21, 140, and 830 μM were observed for $SD_{24}G_{10}$, $SD_{46}G_{10}$ and $SD_{95}G_{10}$, respectively. In particular, the interaction of $SD_{24}G_{10}$ was found to be maximum among all polymers.

A similar type of strategy to bind the trimeric pocket of HA was used to inhibit IAV infection by employing sialyllactose-modified three-way junction DNA (Figure 20).[71] Since DNA offers advantages that allow the design of a well-ordered structure and control of the number, density, and spatial

distribution of the carbohydrate ligands. Keeping the core DNA scaffold sequence the same, several silayllactose residues were presented onto each DNA terminal to optimize the three simultaneous binding to SA binding pockets. The distance between the two adjacent terminal sialyllactose residues was kept around 6 nm which was slightly higher than the two adjacent HA pockets of 4–5 nm. The slightly higher distance was maintained to overcome the effect of a slightly convex HA surface. This rigid three-way junction DNA scaffold with S3 substituents (as shown in Figure 20A) on all three arms was found to maintain appropriate conformation in the process of binding to HA by providing sialyllactose residues a similar arrangement of three SA binding pockets on HA, thus showed the maximum inhibition of influenza. In a further study, authors replaced the O-sialosides with S-sialosides to exclude any degradation due to enzymatic cleavage of O-sialoside from DNA scaffold by the viral neuraminidase as the S-sialosides are hydrolytically stable.[72,73] The synthesized neuraminidase resistant sialosides that contain unnatural S-glycosidic bonds were equally effective for the recognition of HA on the virus surface. The authors further employed a triangular DNA (Figure 20B) as another tripodal DNA scaffold for the symmetric trivalent
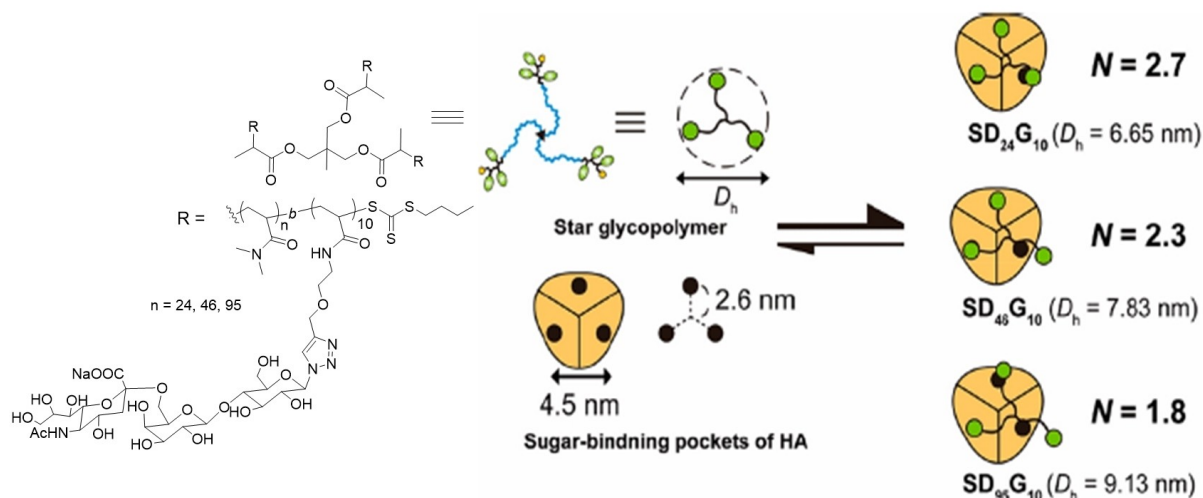
EurJOC
European Journal of Organic Chemistry

Review
doi.org/10.1002/ejoc.202201360

Chemistry
Europe
European Chemical
Societies Publishing

Figure 19. Expected binding modes between the star glycopolymers and HA trimer showing different values of D_h (Hydrodynamic diameter) and N (number of binding sites for each polymer). Polymers of hydrodynamic diameter ~6.65 nm showed maximum interaction because of matched topology with HA trimer binding pockets. Reproduced with permission from Ref. [70]. Copyright (2019), American Chemical Society.
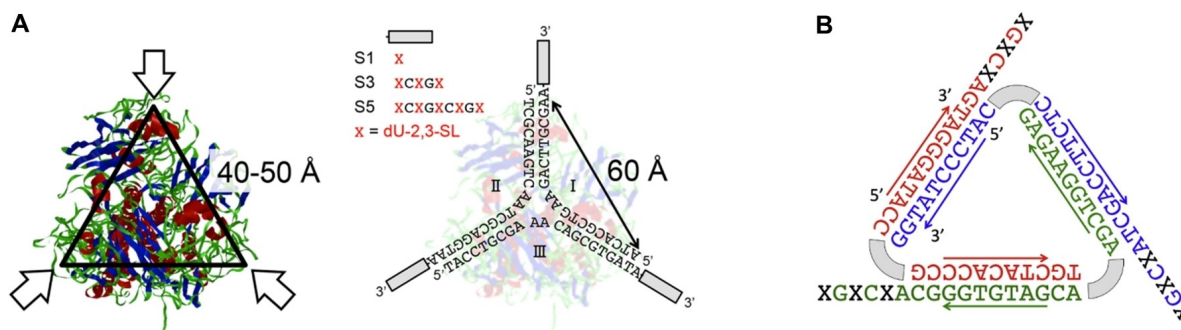

Figure 20. (A) Structural representation of HA trimer and its complex with 2,3-sialyllactose-modified three-way junction DNA. Reproduced with permission from Ref. [71]. Copyright (2018), American Chemical Society; (B) Triangular DNA synthesized by the hybridization of three inverted DNAs. Reproduced with permission from Ref. [74]. Copyright (2019), Elsevier.

presentation of sialyllactose moieties.[74] The scaffold size of the triangular DNA was reduced to 5 nm from 6 nm for a three-way junction and thus ligand presentation of the triangular scaffold matched closely to SA binding sites of HA_3 (~4.2 nm). However, the binding affinity of the triangular scaffold was similar to that of the three-way junction which concluded that a more moderate scaffold size may be needed to achieve binding with convex HA_3. Moreover, fully unfunctionalized and sialyllactose functionalization on one of the three arms did not show any HA inhibition. These results confirmed that there are no unspecific interactions between bare DNA scaffold and HA. Sialyllactose on two and all three arms inhibited HA at 2.0×10^{-6} M and 5.0×10^{-7} M, respectively as determined by hemagglutination assay.

4. Langerin

Langerin is a C-type transmembrane lectin protein expressed on the Langerhans cells, which are immune cells and function more like dendritic cells in antigen recognition. The main function of langerin is to recognize and internalize the pathogen in the Langerhans cells which further stimulates T-cells response through antigen presentation. Langerin consists of an extracellular domain which comprises of a neck region and a carbohydrate recognition domain (CRD) as shown in Figure 21.[75] The neck region of langerin consists of alpha-helices and mediates the formation of langerin homotrimeric structure through coiled-coil interactions. The trimeric structure is essential for the optimal binding to carbohydrate ligands.[76] The crystal structure of the truncated trimeric langerin showed that the multiple interactions between the CRDs and neck region make the trimeric langerin a rigid unit with the three CRDs in fixed positions. The primary sugar binding sites are separated by a distance of around 42 Å.[75] Ligand recognition studies of langerin showed that it binds to highly mannosylated compounds either through terminal non-reducing mannose units or internal Manα1,2-Man units. The binding mode of the non-reducing mannose is similar to the monosaccharide mannose, except that it is 180 degrees flipped by the axis perpendicular to the C3—C4 bond. The binding sites of langerin
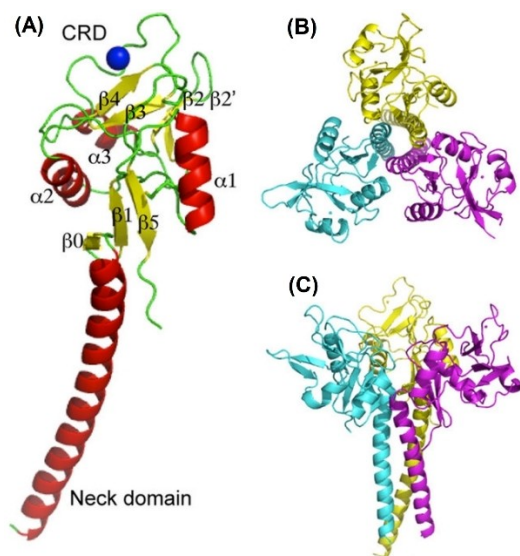
EurJOC
European Journal of Organic Chemistry

Review
doi.org/10.1002/ejoc.202201360

Chemistry Europe
European Chemical
Societies Publishing

Figure 21. (A) Structure of truncated langerin where sheets are shown in yellow, helices in red, loops in green, and Ca^{2+} is shown as a blue ball; (B) Top view of the trimeric structure; (C) Side view of the trimeric structure. Reproduced from Ref. [75], published by Elsevier under a CC-BY license.

are a little extended and can interact with other sugar residues in mannose oligosaccharides.

Langerin was found to be unique among C-type CRDs since it could also interact with N-acetylglucosamine and galactose-based saccharides apart from mannose/fucose units. Several research studies showed that langerin exhibits an unusual binding affinity towards 6-sulfated galactose, a moiety found in keratan sulfate.[77] Ota et al. observed that a disaccharide named as L4, a keratan sulfate component that contains 6-sulfated galactose, and its related compounds are effective ligands for langerin.[78] They chemically synthesized several oligomeric (trimeric and polymeric) derivatives of the L4 ligand to create a new high-affinity binding ligand of langerin. The enzyme-linked immunosorbent assay (ELISA) revealed that the synthesized trivalent ($IC_{50} = 2.7\ \mu M$) and polymeric ($IC_{50} = 2.1$ nM) L4 deriva-

tives found to display over 1000-fold affinity towards langerin as compared to monomeric L4 with IC_{50} of 3.5 mM.

Neuhaus et al. recently reported the synthesis of linear and three-arm branched glycol oligomers and studied their binding with langerin.[79] The chain length of all three ligand-carrying branches was varied independently (symmetrically and unsymmetrically) to obtain an optimized system and a correlation between scaffold size and inhibitory potential against langerin was developed. Binding studies demonstrated that the smallest three-arm scaffold shown in Figure 22 had the highest binding and the stepwise elongation of one, two, or all three arms resulted in decreased binding. Overall, these results suggested that a very high affinity towards langerin can be achieved using an optimized carbohydrate-functionalized trivalent scaffold.

Since langerin binds to a variety of carbohydrates such as fucose, mannose and sulfated sugars. Given this rather broad ligand range and taking into consideration the multitude of the other common lectins such as Mannose Binding Protein, dectin-2, and DC-SIGN binding similar saccharides, it has been challenging to selectively target langerin expressing cells. Recently, Bachem et al. tried to address this challenge by introducing a glycomimetic 2-N-tosyl-aminoglucose (Glc2NTs) moiety as a selective ligand for langerin and demonstrated that the attachment of Glc2NTs to various scaffolds such as liposomes, polymers, and DNA resulted into improved affinity towards langerin.[80,81] In one of their studies, a rationally designed well-defined molecular system was constructed by the hybridization of 39 nucleotide long DNA template strands with three different 13 nucleotide peptide nucleic acid (PNA) strands to obtain DNA-PNA complex as shown in Figure 23C. Among three PNA strands, two were functionalized by Glc2NTs or TriGlc2NTs (trivalent derivative of Glc2NTs) via 1,4-addition of thiolated PNA to maleimide functionality of these ligands. The bivalent functionalization of TriGlc2NTs ligand displaced a remarkable affinity enhancement and the IC_{50} value decreased to $\sim 0.3\ \mu M$ for the bivalent presentation of TriGlc2NTs from ~ 347 mM for the monovalent Glc2NTs as demonstrated by SPR assay. Moreover, the complex Biv-TriGlc2NTs-13 (i.e., doubly functionalized with TriGlc2NTs) provided 100 and 1000-fold
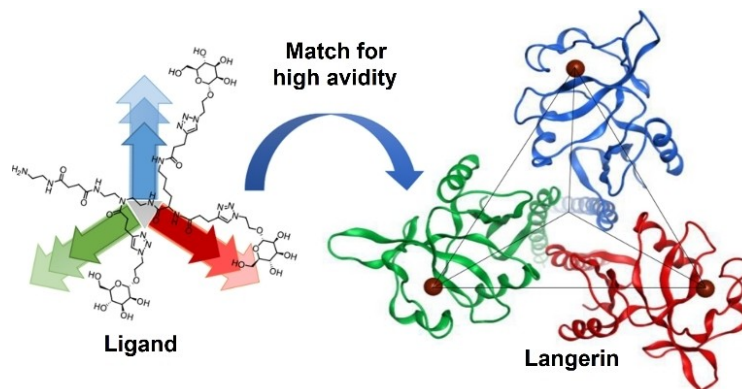

Figure 22. Molecular structure of the trivalent glycooligomer which showed highest binding to langerin extracellular domain (EDC) with interbinding site distance of around 42 Å. Reproduced with permission from Ref. [79]. Copyright (2019), American Chemical Society.
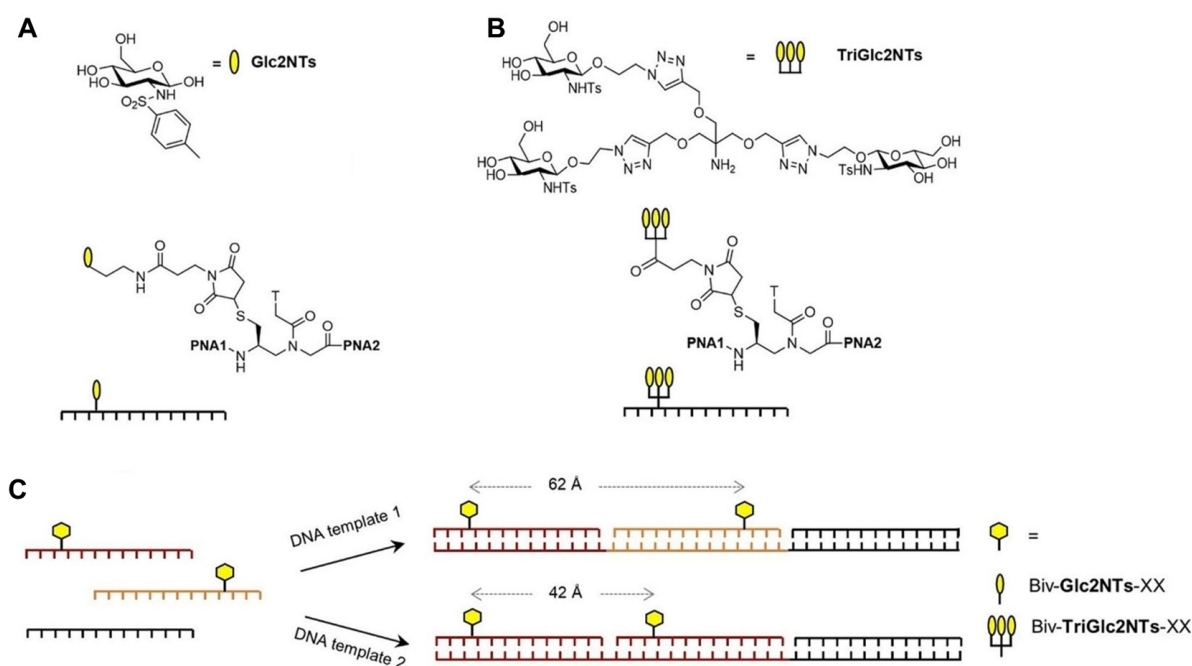
EurJOC
European Journal of Organic Chemistry

Review
doi.org/10.1002/ejoc.202201360

Chemistry Europe
European Chemical
Societies Publishing

Figure 23. (A) Molecular structure of Glc2NTs ligand and its PNA conjugate; (B) Molecular structure of TriGlc2NTs ligand and its PNA conjugate; (C) Hybridization of unmodified (black) and modified (red, orange) PNA oligomers with DNA template strands to obtain PNA-DNA complexes having ligands (yellow) at varied distances. Reproduced from Ref. [81], published by Wiley-VCH under the terms of a CC-BY 4.0 license.

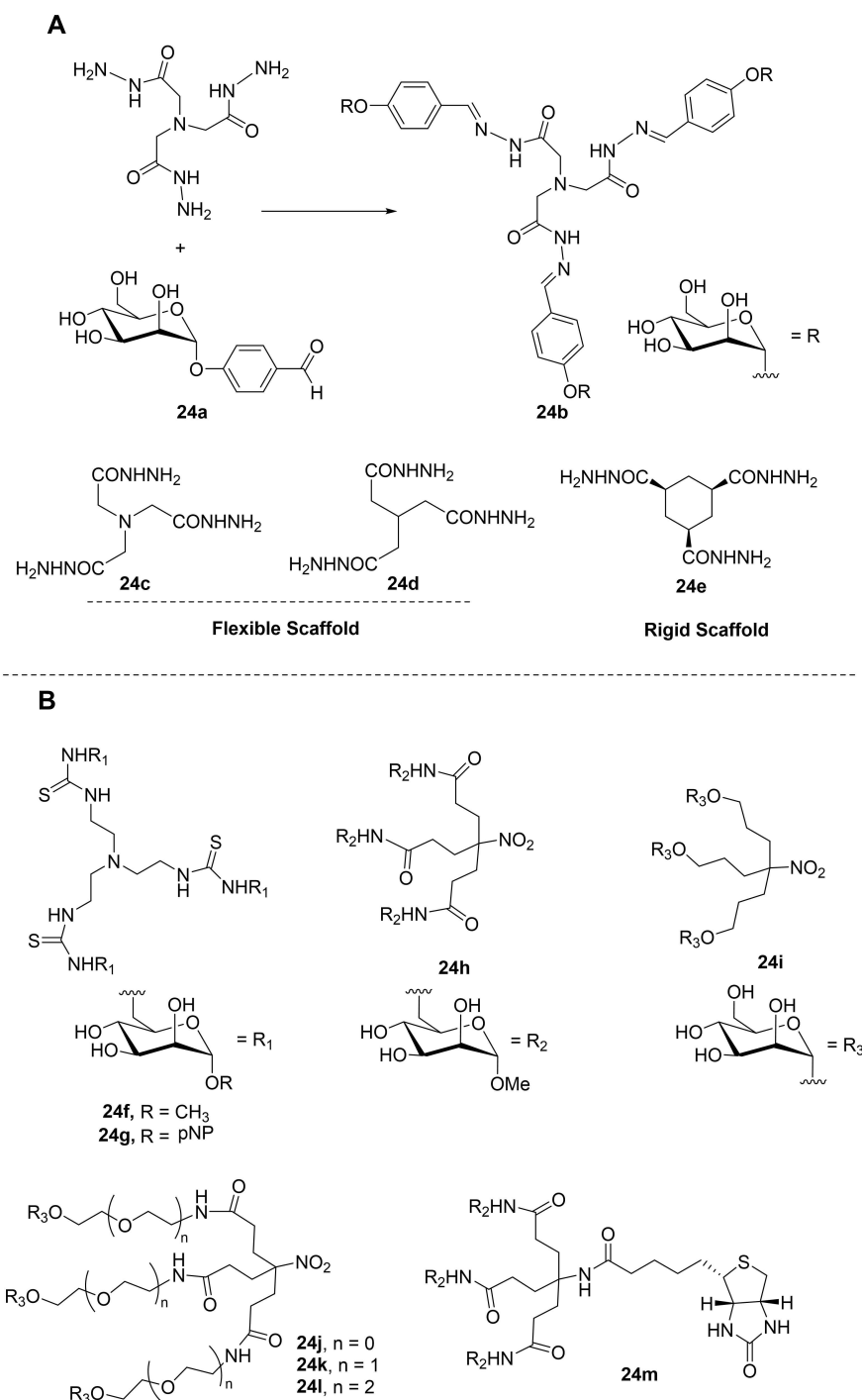higher affinity than TriGlc2NTs and Glc2NTs ligands, respectively.

5. Miscellaneous

Concanavalin A (ConA) is a plant lectin which specifically binds to the various sugars and glycoproteins mainly internal and non-reducing terminal of α-D-mannosyl and α-D-glucosyl groups. ConA is a D_2 symmetric homotetramer and each subunit binds to metal ions (Ca^{2+} and Mn^{2+}). In 2004, Lehn and coworkers[82] prepared a dynamic carbohydrate library from a pool of carbohydrate aldehydes, hydrazine linkers, and scaffolds. The synthesized compounds were used to study the interaction of carbohydrates and lectin with ConA as a target. Among various synthesized glycoconjugates, a more flexible scaffold (**24c** and **24d**) shows higher activity for ConA than the glycoconjugates of rigid scaffold (**24e**, Figure 24A). The mannose was found as the most active carbohydrate. The IC$_{50}$ value of trivalent mannoside (**24b**) was found 22 μM as compared to the methyl-α-D-mannoside (IC$_{50}$ = 0.8 mM).

In 1998, Lindhorst and coworkers[83] synthesized the trivalent mannosides and explore their ability to inhibit the mannose dependent binding of *E. coli* HB 101(pPK14). The trivalent *O*-mannosides **24h** and **24i** were found potent inhibitors for *E. coli* inhibition with IC$_{50}$ 11 and 39 μM, respectively (Figure 24B). However, thiourea linker based trivalent mannosides **24f** and **24g** shows very less inhibition with IC$_{50}$ 5333 μM and 429 μM, respectively. After having the lead trivalent mannoside **24h** in hand, Lindhorst et al.[84] further

explored the structure modification in the aglycone part and the length of the linker. The spacer modified trivalent mannosides **24j**, **24k** and **24l** shows inhibition with IC$_{50}$ value 238, 222, and 134 μM. These results suggest that the positioning of mannose in trivalent mannoside **24h** is better than the trivalent mannosides **24j**, **24k**, and **24l**. The length of the spacer is disrupting the receptor binding with the trivalent mannosides. The most potent trivalent mannoside **24h** with better inhibition capacity was conjugated with biotin to afford biotin conjugated trivalent mannoside **24m** for biological testing.

Adenoviruses belong to the *Adenoviridae* family of viruses which spread infection worldwide in humans as well as other animals. Adenoviruses of serotypes 8, 9, and 37 majorly contribute to severe eye infection EKC (epidemic keratoconjunctivitis). The interactions of adenoviruses with cellular receptors are through homotrimeric fiber proteins. Adenovirus type 37 tends to bind and infect the human corneal cells through sialic acid. Kihlberg and coworkers[85] synthesized the 3′-sialyllactose based multivalent inhibitor of EKC causing adenovirus of serotype 37 (Ad37). 3′-Sialyllactose was conjugated with human serum albumin (HSA) through squaric decyl ester glycoside **25a** (Figure 25A). The binding efficiency of trivalent sialyllactose was not studied for Ad37. In 2011, Elofsson and coworkers[86] synthesized trivalent sialic acid based inhibitors of Ad37 (Figure 25B). The trivalent sialic acid glycotripod **25e** was the most potent and equivalent to 17-valent sialic acid-HSA conjugate. The cell based infection assay was done to evaluate the anti-adenoviral potential and glycotripod **25e** inhibited the infection of HCE cells by Ad37 virions with an IC$_{50}$ value of 0.38 μM. The trivalent compound **25e** was found more

EurJOC
European Journal of Organic Chemistry

Review
doi.org/10.1002/ejoc.202201360

Chemistry
Europe
European Chemical
Societies Publishing

Figure 24. (A) Trivalent mannoside and different kinds of scaffolds for targeting plant lectin ConA; (B) Trivalent mannosides for inhibiting *E. coli*.

potent than sialic acid, 3′-sialyllactose-HSA, and sialic acid-HSA conjugates. In 2015, Elofsson and coworkers[87] synthesized the trivalent sialic acid derivatives (Figure 25C) and explored their inhibitory activity against Adenovirus type 37 (Ad37) infections of human corneal epithelial (HCE) cells.

6. Conclusion and Outlook

This review describes efforts to optimize efficient glycotripods for a significantly high binding with trimeric lectins. Various modification methods have been reported on trivalent scaffolds to broaden its applications as a favorable lectin binder. These useful modifications have been utilized for the construction of tripodal inhibitors for various trivalent lectins. It has been
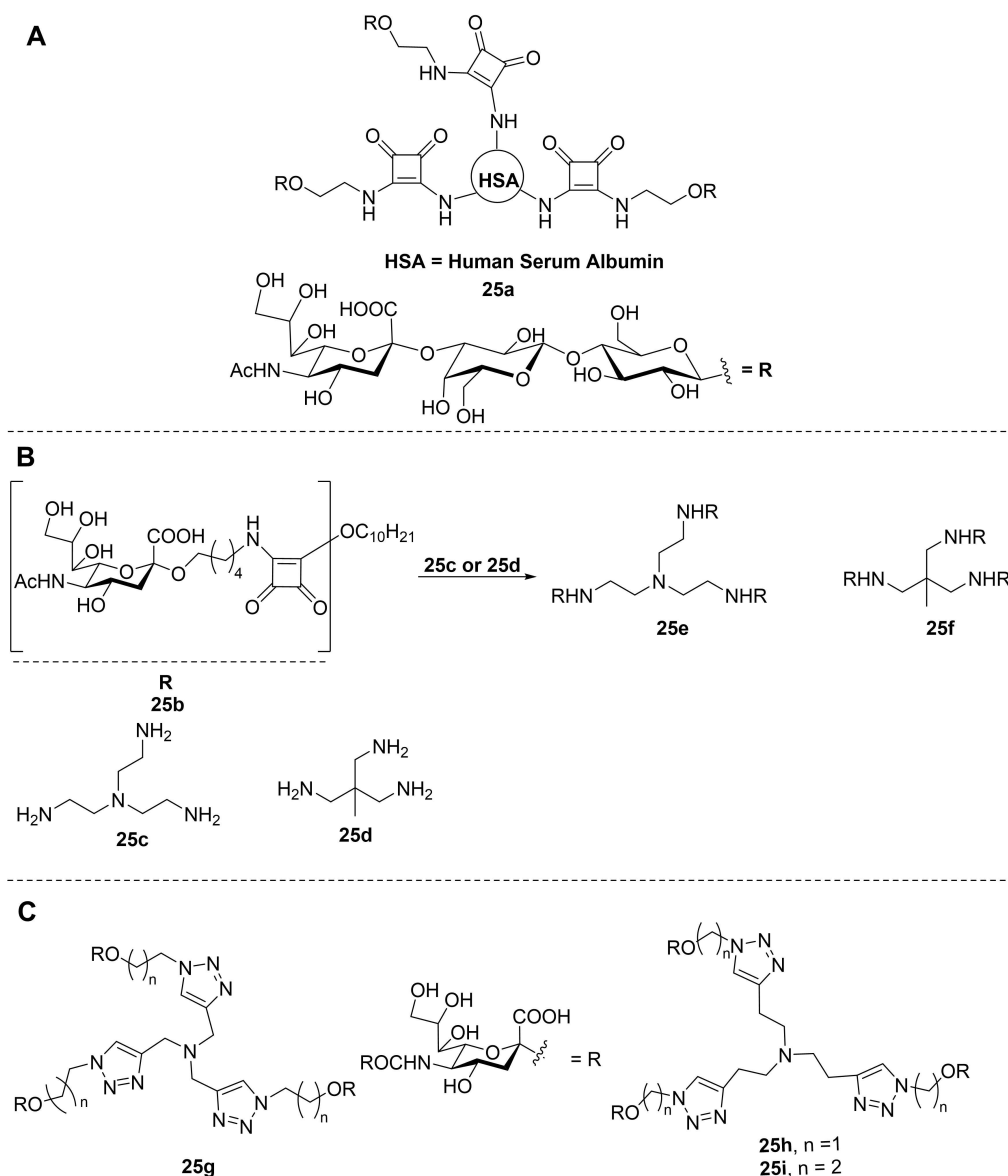
EurJOC
European Journal of Organic Chemistry

Review
doi.org/10.1002/ejoc.202201360

Chemistry
Europe
European Chemical
Societies Publishing

Figure 25. (A) HSA conjugated trivalent sialyllactose; (B) Trivalent sialosides for inhibiting Ad37 virions; (C) Triazole based trivalent sialosides for inhibiting Ad37 virions.

concluded that till now ASGPR is highly specific for *N*-acetylgalactosamine and the optimal spacer length between the main scaffold (branching point) and the sugar residue is found to be 20 Å. This spacer length and sugar led to an increase in the binding affinity of the ligand towards ASGPR. Furthermore, trivalent bicyclic *N*-acetylgalactosamine conjugates show binding affinity in the picomolar range. Hence there is still scope to explore bicyclic sugar as ligands for trivalent glycoconjugates. HA is highly specific for binding with sialic acid while langerin shows selectivity for binding with mannose and sulfated *N*-acetyl galactosamine. In comparison to other multivalent systems, the target specific design and easy modification make them potential candidates as trimeric lectin binders/inhibitors. Much progress has also been accomplished in the last decade to deliver the cargo (genetic material, drugs,

and lipids) with the help of trivalent glycoconjugates. Moreover, the design of tripodal inhibitors has not been fully explored yet. There are still several other possibilities to use new scaffolds and incorporate new functionalities to enhance binding affinity and target specificity so that these controlled systems can be utilized in clinical applications.

Acknowledgements

Conflict of Interest

The authors declare no conflict of interest.

Data Availability Statement

Data sharing is not applicable to this article as no new data were created or analyzed in this study.

[1] a) J. Petterson, R. Nordfelth, E. Dubinina, T. Bergman, M. Gustafsson, K. E. Magnusson, H. W. Watz, *Sciences* **1996**, *273*, 1231–1233; b) A. Imberty, A. Varrot, *Curr. Opin. Struct. Biol.* **2008**, *18*, 567–576.

[2] M. M. Fuster, J. D. Esko, *Nat. Rev. Cancer* **2005**, *5*, 526–542.

[3] A. Varki, R. Cimmings, J. Esko, H. Freeze, G. Hart, J. Marth, *Essentials of Glycobiology*, Cold Spring Harbor Laboratory Press, New York, **1999**.

[4] a) A. Varki, *Glycobiology* **2017**, *27*, 3–49; b) P. Valverde, J. D. Martinez, F. J. Canada, A. Arda, J. J. Barbero, *ChemBioChem* **2020**, *21*, 2999–3025.

[5] Y. C. Lee, R. T. Lee, *Acc. Chem. Res.* **1995**, *28*, 321–327.

[6] S. Bhatia, L. C. Camacho, R. Haag, *J. Am. Chem. Soc.* **2016**, *138*, 8654–8666.

[7] S. Bhatia, M. Dimde, R. Haag, *MedChemComm* **2014**, *5*, 862–878.

[8] C. Fasting, C. A. Schalley, M. Weber, O. Seitz, S. Hecht, B. Koksch, J. Dernedde, C. Graf, E.-W. Knapp, R. Haag, *Angew. Chem. Int. Ed.* **2012**, *51*, 10472–10498; *Angew. Chem.* **2012**, *124*, 10622–10650.

[9] M. Kumari, S. Prasad, L. Fruk, B. Parshad, *Future Med. Chem.* **2021**, *13*, 419–438.

[10] A. Bernardi, J. Jimenez-Barbero, A. Casnati, C. De Castro, T. Darbre, F. Fieschi, J. Finne, H. Funken, K. E. Jaeger, M. Lahmann, T. K. Lindhorst, M. Marradi, P. Messner, A. Molinaro, P. V. Murphy, C. Nativi, S. Oscarson, S. Penades, F. Peri, R. J. Pieters, O. Renaudet, J. L. Reymond, B. Richichi, J. Rojo, F. Sansone, C. Schaffer, W. B. Turnbull, T. Velasco-Torrijos, S. Vidal, S. Vincent, T. Wennekes, H. Zuilhof, A. Imberty, *Chem. Soc. Rev.* **2013**, *42*, 4709–4727.

[11] S. Bhatia, M. Hilsch, J. L. C. Camacho, K. Ludwig, C. Nie, B. Parshad, M. Wallert, S. Block, D. Lauster, C. Bottcher, A. Herrmann, R. Haag, *Angew. Chem. Int. Ed.* **2020**, *59*, 12417–12422; *Angew. Chem.* **2020**, *132*, 12517–12522.

[12] B. Lepenies, J. Lee, S. Sonkaria, *Adv. Drug Delivery Rev.* **2013**, *65*, 1271–1281.

[13] R. Roy, P. V. Murphy, H. J. Gabius, *Molecules* **2016**, *21*, 629.

[14] a) N. Jayaraman, *Chem. Soc. Rev.* **2009**, *38*, 3463–3483; b) Y. Kim, J. Y. Hyun, I. Shin, *Chem. Soc. Rev.* **2021**, *50*, 10567–10593.

[15] C. Muller, G. Despras, T. K. Lindhorst, *Chem. Soc. Rev.* **2016**, *45*, 3275–3302.

[16] X. Huang, J. C. Leroux, B. Castagner, *Bioconjugate Chem.* **2017**, *28*, 283–295.

[17] a) M. Spiess, *Biochemistry* **1990**, *29*, 10009–10018; b) A. Ciechanover, A. L. Schwartz, D. A. Varsat, H. F. Lodish, *J. Biol. Chem.* **1983**, *258*, 9681–9689.

[18] a) U. Treichel, K. H. M. zum Buschemfelde, R. J. Stockert, T. Poralla, G. Gerken, *J. Gen. Virol.* **1994**, *75*, 3021–3029; b) S. Becker, M. Spiess, H. D. Klenk, *J. Gen. Virol.* **1995**, *76*, 393–399.

[19] A. D. Springer, S. F. Dowdy, *Nucleic Acid Ther.* **2018**, *28*, 109–118.

[20] M. A. Shia, H. F. Lodish, *Proc. Natl. Acad. Sci. USA* **1989**, *86*, 1158–1162.

[21] O. Khorev, D. Stokmaier, O. Schwardt, B. Cutting, B. Ernst, *Bioorg. Med. Chem.* **2008**, *16*, 5216–5231.

[22] E. A. L. Biessen, D. M. Beuting, H. C. P. F. Roelen, G. A. van de Marel, J. H. van Boom, T. J. C. van Berkel, *J. Med. Chem.* **1995**, *38*, 1538–1546.

[23] R. T. Lee, Y. C. Lee, *Glycoconjugate J.* **1987**, *4*, 317–328.

[24] W. T. Jiaang, P. H. Tseng, S. T. Chen, *Synlett* **2000**, 797–800.

[25] R. T. Lee, Y. C. Lee, *Bioconjugate Chem.* **1997**, *8*, 762–765.

[26] A. R. P. Valentijn, G. A. van der Marel, L. A. Sliedregt, T. J. van Berkel, E. A. Biessen, J. H. van Boom, *Tetrahedron* **1997**, *53*, 759–770.

[27] E. A. L. Biessen, D. M. Beuting, H. C. P. F. Roelen, G. A. van de Marel, J. H. van Boom, T. J. C. van Berkel, *J. Med. Chem.* **1995**, *38*, 1538–1546.

[28] a) E. A. L. Biessen, H. Vietsch, T. J. C. van Berkel, *Biochem. J.* **1994**, *302*, 283–289; b) E. A. L. Biessen, H. Broxterman, J. H. van Boom, T. J. C. van Berkel, *J. Med. Chem.* **1995**, *38*, 1846–1852.

[29] L. A. J. M. Sliedregt, P. C. N. Rensen, E. T. Rump, P. J. van Santbrink, M. K. Bijsterbosch, A. R. P. M. Valentijn, G. A. van der Marel, J. H. van Boom, T. J. C. van Berkel, E. A. L. Biessen, *J. Med. Chem.* **1999**, *42*, 609–618.

[30] L. Tang, Y. Wu, J. Lu, Z. R. Zhang, J. C. Yang, L. Hai, *Chin. Chem. Lett.* **2007**, *18*, 513–515.

[31] P. C. N. Rensan, S. H. van Leeuwen, L. A. J. M. Sliedregt, T. J. C. van Berkel, E. A. L. Biessen, *J. Med. Chem.* **2004**, *47*, 5798–5808.

[32] R. A. Petrov, S. Y. Maklakova, Y. A. Ivanenkov, S. A. Petrov, O. V. Sergeeva, E. Y. Yamansarov, I. V. Saltykova, I. I. Kireev, I. B. Alieva, E. V. Deyneka, A. A. Sofronova, A. V. Aladinskaia, A. V. Trofimenko, R. S. Yamidanov, S. V. Kovalev, V. E. Kotelianski, T. S. Zatsepin, E. K. Beloglazkina, A. G. Majounga, *Bioorg. Med. Chem. Lett.* **2018**, *28*, 382–387.

[33] R. A. Petrov, S. R. Mefedova, E. Y. Yamansarov, S. Y. Maklakova, D. A. Grishin, E. V. Lopatukhina, O. Y. Burenina, A. V. Lopukhov, S. V. Kovalev, Y. V. Timchenko, E. E. Ondar, Y. A. Ivanenkov, S. A. Evteev, A. N. Vaneev, R. V. Timoshenko, N. L. Klyachko, A. S. Erofeev, P. V. Gorelkin, E. K. Beloglazkina, A. G. Majounga, *Mol. Pharmaceutics* **2021**, *18*, 461–468.

[34] M. Wang, Z. Li, F. Liu, Q. Yi, C. Pu, Y. Li, T. Luo, J. Liang, J. Wang, *J. Med. Chem.* **2021**, *64*, 14793–14808.

[35] Y. Zhou, P. Teng, N. T. Montgomery, X. Li, W. Tang, *ACS Cent. Sci.* **2021**, *7*, 499–506.

[36] S. Palit, S. Banerjee, T. Mahata, S. Niyogi, T. Das, C. S. Mandi, P. Chakrabarti, S. Dutta, *ChemMedChem* **2021**, *16*, 2211–2216.

[37] O. Khorev, D. Stockmaier, O. Schwardt, B. Cutting, B. Ernst, *Bioorg. Chem.* **2008**, *16*, 5216–5231.

[38] S. Y. Maklakova, V. A. Naumenko, A. D. Chuprov, M. P. Mazhuga, N. V. Zyk, E. K. Beloglazina, A. G. Majouga, *Carbohydr. Res.* **2020**, *489*, 107928.

[39] G. S. Reshitko, E. Y. Yamansarov, S. A. Evteev, E. V. Lopatukhina, D. O. Shkil, I. V. Saltykova, A. V. Lopukhov, S. V. Kolvalev, A. N. Lobov, I. V. Kislyakov, O. Y. Burenina, N. L. Klyachko, A. S. Garanina, O. A. Dontsova, Y. A. Ivanenkov, A. S. Erofeev, P. V. Gorelkin, E. K. Beloglazkina, A. G. Majouga, *Bioconjugate Chem.* **2020**, *31*, 1313–1319.

[40] C. A. Sanhueza, M. M. Baksh, B. Thuma, M. D. Roy, S. Dutta, C. Preville, B. A. Chrunyk, K. Beaumont, R. Dullea, M. Ammirati, S. Liu, D. Gebhard, J. E. Finley, C. T. Salatto, A. K. Ahmad, I. Stock, K. Atkinson, B. Reidich, W. Lin, R. Kumar, M. Tu, E. M. Klotz, D. A. Price, S. Liras, M. G. Finn, V. Mascitti, *J. Am. Chem. Soc.* **2017**, *139*, 3528–3536.

[41] A. M. Pujol, M. Cuillel, A. S. Jullien, C. Lebrun, D. Cassio, E. Mintz, C. Gateau, P. Delangle, *Angew. Chem. Int. Ed.* **2012**, *51*, 7445–7448; *Angew. Chem.* **2012**, *124*, 7563–7566.

[42] M. E. Ostergaard, J. Yu, G. A. Kinberger, W. B. Wan, M. T. Migawa, G. Vasquez, K. Schmidt, H. J. Gaus, H. M. Murray, A. Low, E. E. Swayze, T. P. Prakash, P. P. Seth, *Bioconjugate Chem.* **2015**, *26*, 1451–1455.

[43] T. P. Prakash, J. Yu, M. T. Migawa, G. A. Kinberger, W. B. Wan, M. E. Ostergaard, R. L. Carty, G. Vasquez, A. Low, A. Chappell, K. Schmidt, M. Aghajan, J. Crosby, H. M. Murray, S. L. Booten, J. Hsiao, A. Soriano, T. Machemer, P. Cauntay, S. A. Burel, S. F. Murray, H. Gaus, M. J. Graham, E. C. Swayze, P. P. Seth, *J. Med. Chem.* **2016**, *59*, 2718–2733.

[44] T. P. Prakash, M. J. Graham, J. Yu, R. Carty, A. Low, A. Chappell, K. Schmidt, C. Zhao, M. Aghajan, H. F. Murray, S. Riney, S. L. Booten, S. F. Murray, H. Gaus, J. Crosby, W. F. Lima, S. Guo, B. P. Monia, E. E. Swayze, P. P. Seth, *Nucleic Acids Res.* **2014**, *42*, 8796–8807.

[45] P. Bhingardeve, B. R. Madhanagopal, H. Naick, P. Jain, M. Manoharan, K. Ganesh, *J. Org. Chem.* **2020**, *85*, 8812–8824.

[46] J. K. Nair, J. L. S. Willoughby, A. Chan, K. Charisse, M. R. Alam, Q. Wang, M. Hoekstra, P. Kandasamy, A. V. Kel'in, S. Milstein, N. Taneja, J. O'shea, S. Shaikh, L. Zhang, R. J. van der Sluis, M. E. Jung, A. Akinc, R. Hutabarat, S. Kuchimanchi, K. Fitzgerald, T. Zimmermann, T. J. C. van Berkel, M. A. Maier, K. G. Rajeev, M. Manoharan, *J. Am. Chem. Soc.* **2014**, *136*, 16958–16961.

[47] R. J. Holland, K. Lam, X. Ye, A. D. Martin, M. C. Wood, L. Palmer, D. Fraser, K. McClintock, S. Majeski, A. Jarosz, A. C. H. Lee, E. P. Thi, A. Judge, J. Heyes, *Mol. Ther.* **2021**, *29*, 2910–2919.

[48] K. Schmidt, T. P. Prakash, A. J. Donner, G. A. Kinberger, H. J. Gaus, A. Low, M. E. Ostergaard, M. Bell, E. E. Swayze, P. P. Seth, *Nucleic Acids Res.* **2017**, *45*, 2294–2306.

[49] K. G. Rajeev, J. K. Nair, M. Jayaraman, K. Charisse, N. Taneja, J. O'Shea, J. L. S. Willoughby, K. Yucius, T. Nguyen, S. S. Morskaya, A. Liebow, W. Querbes, A. Borodovsky, K. Fitzgerald, M. A. Maier, M. Manoharan, *ChemBioChem* **2015**, *16*, 903–908.

[50] A. Mishra, T. R. Castaneda, E. Bader, B. Elshorst, S. Cummings, P. Scherer, D. S. Bangarri, C. Loewe, H. Schreuder, C. Poverlein, M. Helms, S. Jones,

G. Zech, T. Licher, M. Wagner, M. Schudok, M. de Hoop, A. T. Plowright, J. Atzrodt, A. Kannt, I. Laitinen, V. Derdau, *Adv. Sci.* **2020**, *7*, 2002997.

[51] I. Papp, C. Sieben, K. Ludwig, M. Roskamp, C. Bittcher, S. Schlecht, A. Herrmann, R. Haag, *Small* **2010**, *6*, 2900–2906.

[52] R. W. H. Ruigrok, L. J. Calder, S. A. Wharton, *Virology* **1989**, *173*, 311–316.

[53] R. W. H. Ruigrok, P. J. Andree, R. A. M. H. Van Huysduynen, J. E. Mellema, *J. Gen. Virol.* **1984**, *65*, 799–802.

[54] C. Nie, B. Parshad, S. Bhatia, C. Cheng, M. Stadtmüller, A. Oehrl, Y. Kerkhoff, T. Wolff, R. Haag, *Angew. Chem. Int. Ed.* **2020**, *132*, 15662–15666.

[55] M. N. Stadtmueller, S. Bhatia, P. Kiran, M. Hilsch, V. R. Scherer, L. Adam, B. Parshad, M. Budt, S. Klenk, K. Sellrie, D. Lauster, P. H. Seeberger, C. P. R. Hackenberger, A. Herrmann, R. Haag, T. Wolff, *J. Med. Chem.* **2021**, *64*, 12774–12789.

[56] M. Mammen, S. K. Choi, G. M. Whitesides, *Angew. Chem. Int. Ed.* **1998**, *37*, 2755–2794.

[57] C. Nie, M. Stadtmüller, B. Parshad, M. Wallert, V. Ahmadi, Y. Kerkhoff, S. Bhatia, S. Block, C. Cheng, T. Wolff, R. Haag, *Sci. Adv.* **2021**, *7*, eabd3803.

[58] W. J. Lees, A. Spaltenstein, J. E. Kingery-Wood, G. M. Whitesides, *J. Med. Chem.* **1994**, *37*, 3419–3433.

[59] J. E. Kingery-Wood, K. W. Williams, G. B. Sigal, G. M. Whitesides, *J. Am. Chem. Soc.* **1992**, *114*, 7303–7305.

[60] A. Mittal, K. Aarti, S. Prasad, P. K. Mishra, S. K. Sharma, B. Parshad, *Mater Adv* **2021**, *2*, 3459–3473.

[61] B. Parshad, S. Prasad, S. Bhatia, A. Mittal, Y. Pan, P. K. Mishra, S. K. Sharma, L. Fruk, *RSC Adv.* **2020**, *10*, 42098–42115.

[62] B. Parshad, P. Yadav, Y. Kerkhoff, A. Mittal, K. Achazi, R. Haag, S. K. Sharma, *New J. Chem.* **2019**, *43*, 11984–11993.

[63] M. Waldmann, R. Jirmann, K. Hoelscher, M. Weinke, F. C. Niemeyer, D. Rehders, B. Meyer, *J. Am. Chem. Soc.* **2014**, *136*, 783–788.

[64] S. Kosono, A. Kasai, S. Komaba, T. Matsubara, T. Sato, D. Takahashi, K. Toshima, *Chem. Commun.* **2018**, *54*, 7467–7470.

[65] W. Lu, W. Du, V. J. Somovilla, G. Yu, D. Haksar, E. De Vries, G. .-J. Boons, R. P. De Vries, C. A. M. De Haan, R. J. Pieters, *J. Med. Chem.* **2019**, *62*, 6398–6404.

[66] F. Feng, N. Miura, N. Isoda, Y. Sakoda, M. Okamatsu, H. Kida, S.-I. Nishimura, *Bioorg. Med. Chem. Lett.* **2010**, *20*, 3772–3776.

[67] T. Ohta, N. Miura, N. Fujitani, F. Nakajima, K. Niikura, R. Sadamoto, C. T. Guo, Y. Suzuki, K. Monde, S. I. Nishimura, *Angew. Chem. Int. Ed.* **2003**, *42*, 5186–5189; *Angew. Chem.* **2003**, *115*, 5344–5347.

[68] P. Kiran, S. Bhatia, D. Lauster, S. Aleksić, C. Fleck, N. Peric, W. Maison, S. Liese, B. G. Keller, A. Herrmann, *Chem. Eur. J.* **2018**, *24*, 19373–19385.

[69] S. Liese, M. Gensler, S. Krysiak, R. Schwarzl, A. Achazi, B. Paulus, T. Hugel, J. P. Rabe, R. R. Netz, *ACS Nano* **2017**, *11*, 702–712.

[70] M. Nagao, T. Matsubara, Y. Hoshino, T. Sato, Y. Miura, *Bioconjugate Chem.* **2019**, *30*, 1192–1198.

[71] M. Yamabe, K. Kaihatsu, Y. Ebara, *Bioconjugate Chem.* **2018**, *29*, 1490–1494.

[72] M. Yamabe, A. Fujita, K. Kaihatsu, Y. Ebara, *Carbohydr. Res.* **2019**, *474*, 43–50.

[73] S. Bhatia, D. Lauster, M. Bardua, K. Ludwig, S. Angioletti-Uberti, N. Popp, U. Hoffmann, F. Paulus, M. Budt, M. Stadtmüller, T. Wolff, A. Hamann, C. Bottcher, A. Herrmann, R. Haag, *Biomaterials* **2017**, *138*, 22–34.

[74] M. Yamabe, K. Kaihatsu, Y. Ebara, *Bioorg. Med. Chem. Lett.* **2019**, *29*, 744–748.

[75] H. Feinberg, A. S. Powlesland, M. E. Taylor, W. I. Weis, *J. Biol. Chem.* **2010**, *285*, 13285–13293.

[76] N. S. Stambach, M. E. Taylor, *Glycobiology* **2003**, *13*, 401–410.

[77] H. Tateno, K. Ohnishi, R. Yabe, N. Hayatsu, T. Sato, M. Takeya, H. Narimatsu, J. Hirabayashi, *J. Biol. Chem.* **2010**, *285*, 6390–6400.

[78] F. Ota, T. Hirayama, Y. Kizuka, Y. Yamaguchi, R. Fujinawa, M. Nagata, H. S. Ismanto, B. Lepenies, J. Aretz, C. Rademacher, P. H. Seeberger, T. Angata, S. Kitazume, K. Yoshida, T. Betsuyaku, K. Kida, S. Yamasaki, N. Taniguchi, *Biochim. Biophys. Acta Gen. Subj.* **2018**, *1862*, 1592–1601.

[79] K. Neuhaus, E.-C. Wamhoff, T. Freichel, A. Grafmüller, C. Rademacher, L. Hartmann, *Biomacromolecules* **2019**, *20*, 4088–4095.

[80] E. C. Wamhoff, J. Schulze, L. Bellmann, M. Rentzsch, G. Bachem, F. F. Fuchsberger, J. Rademacher, M. Hermann, B. Del Frari, R. van Dalen, D. Hartmann, N. M. van Sorge, O. Seitz, P. Stoitzner, C. Rademacher, *ACS Cent. Sci.* **2019**, *5*, 808–820.

[81] G. Bachem, E.-C. Wamhoff, K. Silberreis, D. Kim, H. Baukmann, F. Fuchsberger, J. Dernedde, C. Rademacher, O. Seitz, *Angew. Chem. Int. Ed.* **2020**, *59*, 21016–21022; *Angew. Chem.* **2020**, *132*, 21202–21208.

[82] O. Ramstrom, S. Lohmann, T. Bunyapaiboonsri, J. M. Lehn, *Chem. Eur. J.* **2004**, *10*, 1711–1715.

[83] S. Kotter, U. K. Wenzel, S. Ehlers, T. K. Lindhorst, *J. Chem. Soc. Perkin Trans. 1* **1998**, 2193–2200.

[84] T. K. Lindhorst, S. Kotter, U. K. Wenzel, S. Ehlers, *J. Chem. Soc. Perkin Trans. 1* **2001**, 823–831.

[85] S. M. C. Johansson, N. Arnberg, M. Elofsson, G. Wadell, J. Kihlberg, *ChemBioChem* **2005**, *6*, 358–364.

[86] S. Spjut, W. Qian, J. Bauer, R. Storm, L. Frangsmyr, T. Stehle, N. Arnberg, M. Elofsson, *Angew. Chem. Int. Ed.* **2011**, *50*, 6519–6521; *Angew. Chem.* **2011**, *123*, 6649–6651.

[87] R. Caraballo, M. Saleeb, J. Bauer, M. Liaci, N. Chandra, R. J. Storm, L. Frangsmyr, W. Qian, T. Stehle, N. Arnberg, M. Elofsson, *Org. Biomol. Chem.* **2015**, *13*, 9194–9205.